AN ANALYSIS OF THE PHOTOELECTRON AND RYDBERG STATES OF FORMALDEHYDE

BY

Carol R. Lessard B.Sc.

A thesis submitted to the Department of Chemistry
in partial fulfillment of the requirements for
the degree of Master of Science.

Brock University
St. Catharines, Ontario

April, 1975

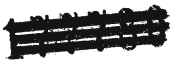

Abstract

Although it is generally accepted that Rydberg orbitals are very large and diffuse, and that electron promotion to a Rydberg orbital is not too different from ionization of the molecule, analysis of the two types of transitions proves otherwise. The photoelectron spectrum of the $^2B_2(n)$ ion has very little vibrational structure attached to the origin band; on the other hand, several of the Rydberg transitions which involve the promotion of the $n(b_2)$ electron exhibit a great deal of vibrational activity. In particular, the members of the n=3 Rydberg series interact with and perturb each other through pseudo-Jahn-Teller vibronic coupling. The vacuum ultraviolet spectrum contains a number of features which are difficult to explain, and two unusually sharp bands can only be identified as representing some form of electron promotion in formaldehyde.

Acknowledgements

First and foremost I would like to thank my supervisor, Dr. D. C. Moule. He has ught me a great deal about molecular spectroscopy and has made this project both interesting and relevant.

I would like to thank Dr. Rothstein for his guidance in the art of computer programming. I would also like to thank the other members of the Chemistry Department for their advice and help with various aspects of my project.

Special thanks go to the National Research Council for their scholarship and to the Chemistry Department for their financial support.

I would like to thank Dr. D. W. Turner for permission to reproduce his results for the photoelectron spectra of H_2CO and D_2CO.

I would also like to thank Dr. S. Bell, of the University of Dundee, Scotland, who kindly provided additional spectra of the $D_2C^{13}O$ isotope for our study.

I wish to acknowledge the assistance of my typist, Janet Hastie, and the technical staff in the completion of this project.

Finally, I wish to thank my husband, Mike, for providing support and encouragement whenever I needed it most.

Table of Contents

Table of Contents (cont'd)

List of Tables

List of Figures

Chapter 1

Introduction

Since its identification in the flame spectra of a number of ethers, aldehydes and other similar molecules (1), formaldehyde has been extensively studied and often used as a basis of analogy for surveys in the field of molecular electronic spectroscopy. There are a number of reasons for this, all of which pertain to the composition and structure of the molecule. It is the smallest molecule containing the carbonyl chromophore, and because there are only four atoms and six fundamental frequencies, the assignment of the vibrational-vibronic transitions in the carbonyl group is a tractable, although complex, problem. In addition, the rotational constants are such that in the electronic transitions which lie in the near ultraviolet, individual line structure can be cleanly resolved and a complete analysis of the excited states can be undertaken. Finally, isotopic data for HDCO, D_2CO and $D_2C^{13}O$ are readily available and are essential for testing vibrational and rotational assignments as well as providing additional spectroscopic parameters from which structural and dynamical information can be extracted.

We shall use the notation recommended by the Joint Commission on Spectroscopy of the IAU and the IUPAC (2), and label the C=O bond as being oriented in the z-direction, so that the x-axis is out of the plane of the molecule, since formaldehyde is planar in its ground state. The molecule has three elements of symmetry in addition to the identity element, i.e., a C_2 axis of rotation along the C=O bond, a σ_v reflection plane in the xz plane including the C=O bond, and a σ_v

reflection plane in the yz plane, including the entire molecule. The symmetry group is C_{2v} and the molecular orbitals belong to one of the four species A_1, A_2, B_1 or B_2. This information is summarized in Table 1 and Figure 1. We note here the confusion of notation in some older papers due to the fact that the molecule was originally oriented in the xz plane, with C=O bond along the z-axis. With this orientation, the B_1 and B_2 designations are reversed.

The most accurate structural determination for formaldehyde comes from the work of Takagi and Oka (3). From an extensive analysis of the microwave spectra of H_2CO, $H_2C^{13}O$, H_2CO^{18}, HDCO and D_2CO, after having made corrections for vibrational as well as electronic interaction, these authors obtained as the ground state structure of formaldehyde the following: $\alpha(HCH) = 116° 31'$, $R(CH) = 1.116\text{Å}$, $R(CO) = 1.208\text{Å}$. Also from this work, we have the rotational constants $A = 9.4096\ cm^{-1}$, $B = 1.2954\ cm^{-1}$, and $C = 1.1342\ cm^{-1}$. The detailed vibrational analysis of formaldehyde comes from a variety of sources (4a-d). Nakagawa, Kashiwagi, Kurihara, and Morino (4e) have analyzed the infrared spectrum in terms of the six fundamental frequencies. Job, Sethuraman and Innes (5) have obtained similar information from an analysis of the hot band structure which is contained on the low-frequency side of the $n \rightarrow \pi^*$ transition. The combined data for the three isotopes are collected in Table 2.

Simple molecular orbital wavefunctions for H_2CO may be obtained from a linear combination of atomic 1s(H), 2s(O), $2p_x(O)$, $2p_y(O)$, $2p_z(O)$, 2s(C), $2p_x(C)$, $2p_y(C)$, and $2p_z(C)$ wave functions which satisfy the symmetry requirements of the C_{2v} point group. The MO's of lowest energy which are obtained from the LCAO-MO scheme are a pair labelled $a_1$1s(C) and $a_1$1s(O). These do not contribute to the valence structure

Figure 1

(a) Geometry of Formaldehyde in the Ground State (ref.3)
and Usual Orientation

(b) Six Normal Vibrations of Formaldehyde in the Ground State (ref.4b)

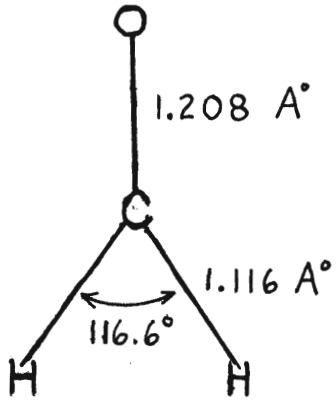

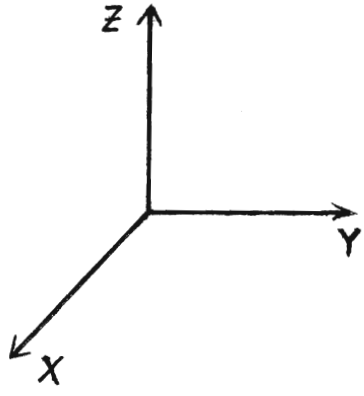

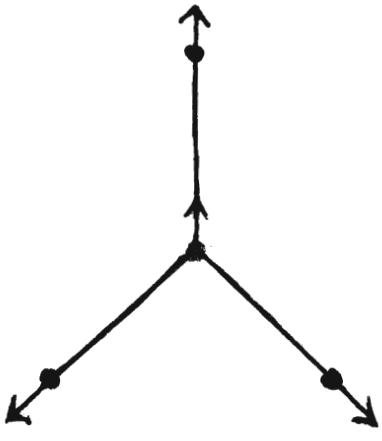

$\nu_1 (a_1)$

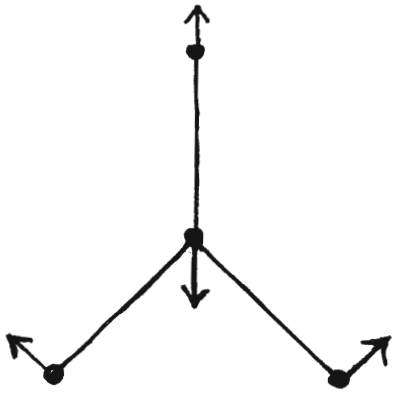

$\nu_2 (a_1)$

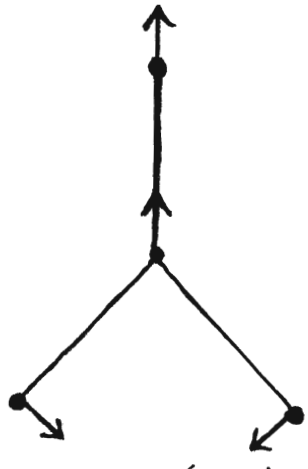

$\nu_3 (a_1)$

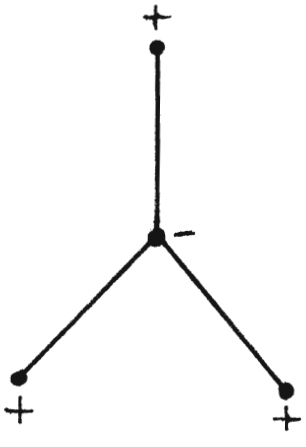

$\nu_4 (b_1)$

$\nu_5 (b_2)$

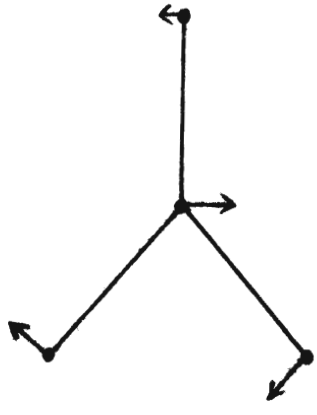

$\nu_6 (b_2)$

Table 1

Symmetry Species and Character Table for the C_{2v} Point Group

	E	$C_2(z)$	$\sigma_v(xz)$	$\sigma_v'(yz)$	
A_1	1	1	1	1	T_z
A_2	1	1	-1	-1	R_z
B_1	1	-1	1	-1	T_x, R_y
B_2	1	-1	-1	1	T_y, R_x

Table 2

Ground State Vibrational Frequencies for Formaldehyde(cm^{-1})

(ref. 5)

	H_2CO	HDCO	D_2CO
ν_1	2766.4	2844.1	2055.8
ν_2	1746.1	1723.4	1700
ν_3	1500.6	1400.6	1105.7
ν_4	1167.3	1059	933.8
ν_5	2843.4	2120.7	2159.7
ν_6	1251.2	1027	990.4

and may be regarded as nonbonding orbitals on the carbon and oxygen centres. A MO which bears the description $a_1\sigma(CO)$ is the next lowest in energy and is formed from the in-phase overlap of the 2s and $2p_z$ AO's of carbon and oxygen. Following this is a pair of group orbitals $a_1\sigma(CH)$ and $b_2\sigma(CH)$ which result from the in-plane symmetric and anti-symmetric combinations of the 1s(H) AO's of the two hydrogens with the 2s and 2p orbitals on carbon. The next orbital is labelled $a_1n\sigma(CO)$. It may be considered to be constructed as a $2s-2p_z(O)$ hybrid MO on the oxygen, and is referred to as either a weak $\sigma(CO)$ bonding orbital or as a second nonbonding orbital n(CO)--hence the notation $n\sigma(CO)$. Slightly above this lies the $b_1\pi(CO)$ orbital which is formed from the in-phase overlap of the $2p_x(C)$ and $2p_x(O)$ AO's. This is the orbital which is usually referred to as the π bond. The last stable orbital can be described as a non-bonding $b_2n(O)$ orbital. In its properties, it approximates rather closely to the $p_y(O)$ AO. The antibonding orbitals $b_1\pi^*(CO)$, $a_1\sigma^*(CH)$, $b_2\sigma^*(CH)$ and $a_1\sigma^*(CO)$ follow in increasing order. If we place the twelve valence electrons into the six lowest energy levels, we obtain the following ground state electronic configuration:

$$(3a_1)^2(4a_1)^2(1b_2)^2(5a_1)^2(1b_1)^2(2b_2)^2$$

Schematic representations of these orbitals are shown in Figure 2.

A number of qualitative predictions about the molecular configurations of formaldehyde in its various excited states were successfully made by Walsh (6), who considered the correlation of the one-electron orbital energies with the changing out-of-plane angle. The primary postulate on which his diagram is based is that a molecular orbital has a lower energy (i.e., contains an electron which is more tightly bound) if, on changing the bond angle at the atomic center, the MO

Figure 2

The Molecular Orbitals and Intravalence Electronic Transitions for Formaldehyde (ref.33)

a_1 b_1 b_2

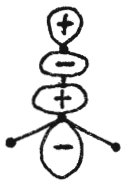

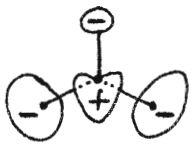

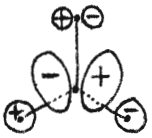

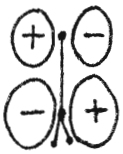

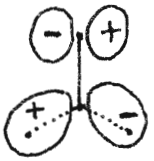

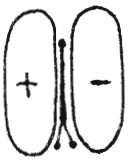

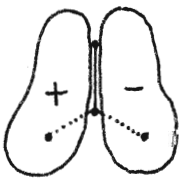

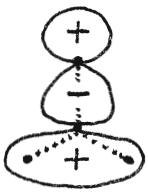

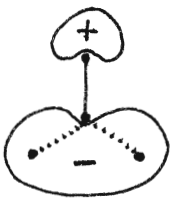

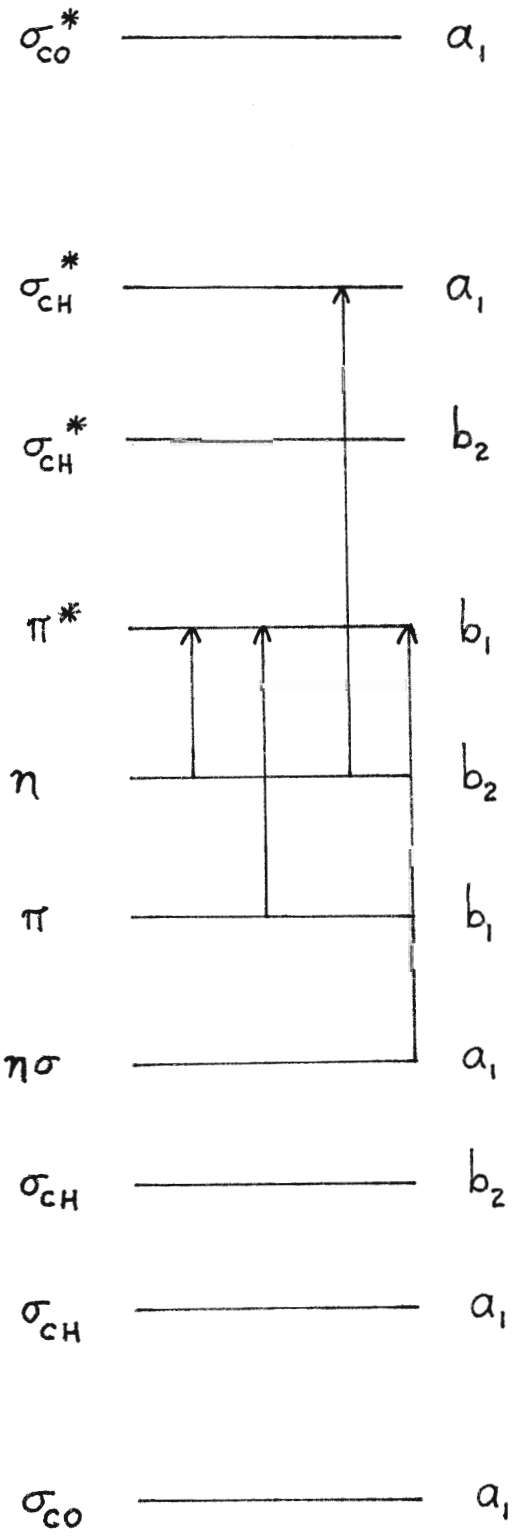
σ_{CO}^* a_1
σ_{CH}^* a_1
σ_{CH}^* b_2
π^* b_1
n b_2
π b_1
$n\sigma$ a_1
σ_{CH} b_2
σ_{CH} a_1
σ_{CO} a_1

changes from being a p-type orbital to being built from an s-type AO. In Figure 3 the effect of such a distortion is considered. A significant feature of the out-of-plane bending is that the $C_2(z)$ and σ_{yz} elements of symmetry which are present in the planar form are removed, and the wavefunctions must now be classified under the operations of the C_s point group. From the diagram we see that only one orbital, the π^*(CO) MO, becomes more binding with increasing nonplanar distortion; all of the remaining orbitals are adversely affected to some degree. It follows that only those electronic configurations which occupy the $b_1\pi^*$(CO) level will display any tendency towards nonplanarity. Of the singlet states, only the $^1A_2(n, \pi^*)$, $^1A_1(\pi, \pi^*)$ and $^1B_1(n\sigma, \pi^*)$ states should be non-planar. This correlation of one-electron states was confirmed by Brand (7) in 1956 who demonstrated from a detailed analysis of the vibronic structure of $\tilde{A}^1A_2(n, \pi^*) \leftarrow \tilde{X}^1A_1$ transition that the nuclear configuration of the upper state was indeed distorted from the molecular plane.

In addition to the valence-shell orbitals which we have discussed above, there are a large number of higher-energy orbitals referred to as Rydberg orbitals. These arise from electronic configurations in which one electron is promoted to an orbital with a principal quantum number n greater than the maximum ground state value. These orbitals become more like atomic orbitals as n increases, and they give rise to a series of Rydberg states which converge at a limit corresponding to the complete removal of the electron. To a good approximation the energies of the Rydberg states can be represented by the formula:

$$E_R = A - \frac{R}{(n - \delta)^2}$$

Figure 3

Walsh Diagram for Formaldehyde

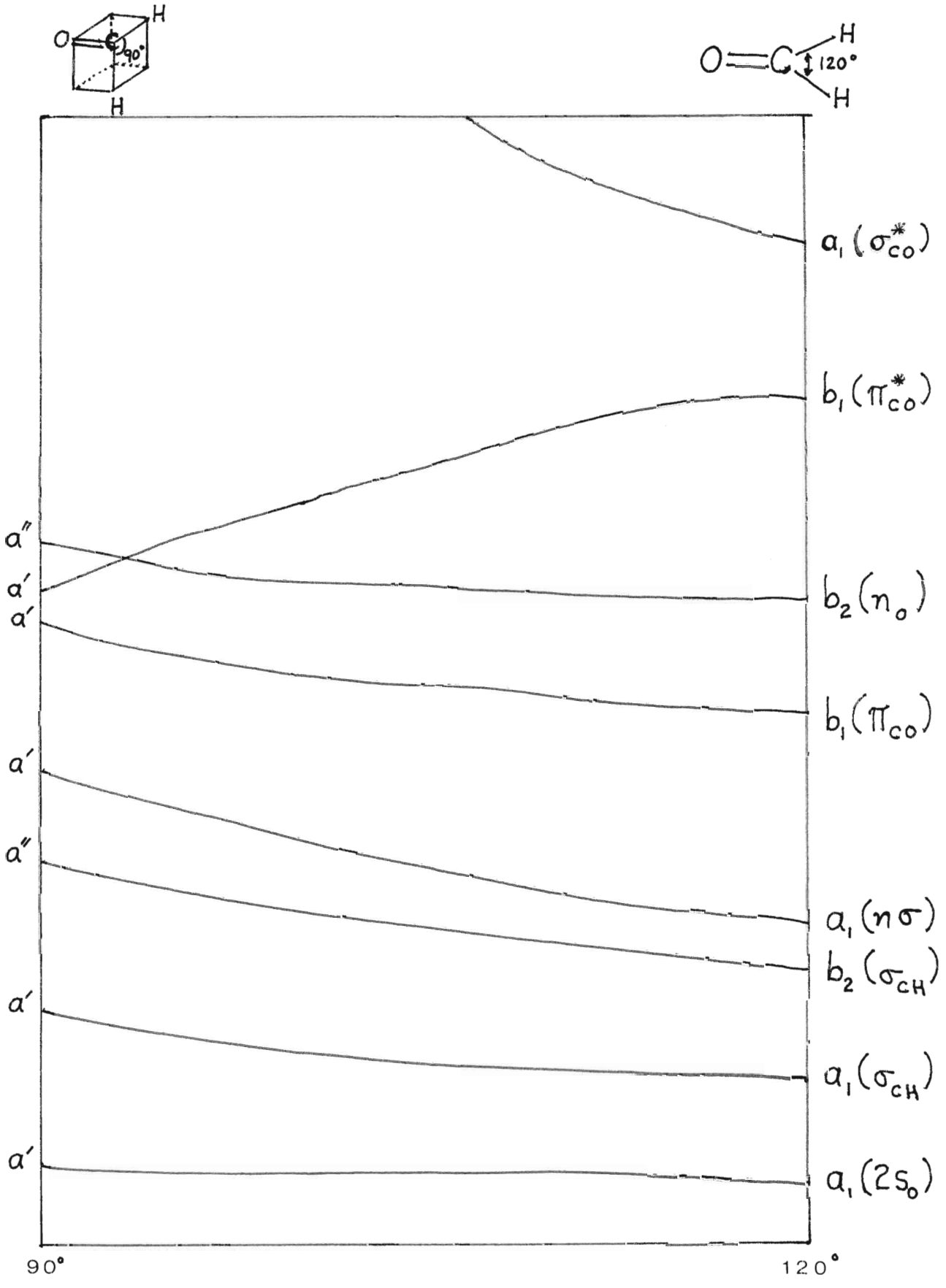
O
H
90°
H
O
C
H
120°
H
$a_1(\sigma^*_{CO})$
$b_1(\pi^*_{CO})$
a''
a'
$b_2(n_O)$
a'
$b_1(\pi_{CO})$
a'
a''
$a_1(n\sigma)$
$b_2(\sigma_{CH})$
a'
$a_1(\sigma_{CH})$
a'
$a_1(2s_O)$
90°
120°
H C H Angle

where A is the ionization limit

n is the principal quantum number

δ is the quantum defect.

For molecules containing only first row elements, values for δ are well-established.

$\delta < 0.1$ for nd electrons

$= 0.3$ to 0.5 for np electrons

$= 0.9$ to 1.2 for ns electrons

Although Rydberg orbitals are generally considered not to mix with valence shell orbitals, for small values of n their transition energies are of the same magnitude as some of the valence shell transition energies, and they must be included in a complete molecular orbital model of formaldehyde.

Chapter 2

Theory

(A) The CNDO/2 Program

Within the last ten years, there has developed a new interest in evaluating the electronic states of a number of small molecules, including formaldehyde. Table 3 lists a number of these calculations for intravalence transitions and illustrates the variety of molecular orbital approximations which have been used. The first eight columns are concerned with semi-empirical calculations such as PPP, CNDO/1, CNDO/2, etc., while the remainder of the table refers to ab initio results from PCMO, CI and other techniques.

In view of the success of the above calculations in predicting the positions of intravalence electronic transitions, we felt that it would be useful to extend the available information to include Rydberg and ionic states. According to Buenker and Peyerimhoff (8), certain molecular structural parameters, namely bond angles, are predicted as accurately if not more accurately by CNDO/2 technique than they are by ab initio treatments.

The CNDO/2 program has been designed to construct a basis set of molecular orbitals from a minimum number of valence atomic orbitals. For formaldehyde, these atomic orbitals are 1s(H), 1s(H), 2s(C), $2p_x$(C), $2p_y$(C), $2p_z$(C), 2s(O), $2p_x$(O), $2p_y$(O), and $2p_z$(O), and as we have seen earlier, the resulting set of molecular orbitals is:

$$\sigma_{CO}(a_1)\sigma_{CH}(a_1)\sigma_{CH}(b_2)n\sigma(a_1)\pi(b_1)n(b_2)\pi^*(b_1)\sigma^*_{CH}(b_2)\sigma^*_{CH}(a_1)\sigma^*_{CO}(a_1)$$

Hence, in its original form, the CNDO/2 program is capable of evaluating all of the intravalence electronic transitions as well as the ionic states of H_2CO using the virtual orbital approximation.

Table 3 Comparison of the Calculated Transition Energies (ev) for Formaldehyde

	Semi-empirical								Ab initio						
reference	(38)	(39)	(40)	(41)	(42)	(42)	(42)	(43)	(44)	(44)	(8)	(15)	(14)	(45)	(31)
$^1A_2(n,\pi^*)$	4.1	3.5	3.8	3.5	4.6	4.7	3.8	3.6	3.5	3.6	3.4	3.8	3.8		
$^1B_2(n,\sigma^*)$	6.4	8.6			10.3	10.4	8.1	8.1	17	17	10.4				
$^1B_1(n\sigma,\pi^*)$		10.0			8.9	9.1	8.3	9.1	8.6	8.9	8.6	9.4	9.0		8.4
$^1A_1(\pi,\pi^*)$	8.2	9.8	7.4	8.1	11.6	11.8	15.6	9.6	11.2	12.0	12.1	11.3	11.4	9.9	9.8
$^3A_2(n,\pi^*)$	3.7	3.5	3.6	2.7	4.0	4.1	3.5		2.1	2.3	3.0	3.4	3.4		
$^3B_2(n,\sigma^*)$	6.4	8.6			8.0	8.3					10.0				
$^3B_1(n\sigma,\pi^*)$		8.9			7.8	8.1			6.5	7.0	7.6		8.1		
$^3A_1(\pi,\pi^*)$	4.8	5.4	5.1	4.0	5.7	7.2				3.9	5.0	5.7	5.6		

(B) CNDO Modifications--Rydberg Orbitals

Although the program developed by Pople, Santry and Segal (9) (hereafter referred to as PSS) is capable of handling open-shell configuration problems, it was not designed to operate with excited-state configurations other than those obtained by promoting an electron from the highest occupied ground state orbital to the lowest unoccupied orbital. In order to describe the Rydberg orbitals, it is necessary to expand the valence set of molecular orbitals to include nine new atomic orbitals, s, p_x, p_y, p_z, d_{xy}, d_{xz}, d_{yz}, $d_{x^2 - y^2}$ and d_{z^2}. The assignment of a principal quantum number to these orbitals poses a problem, since it is only for the higher states that the Rydberg orbitals resemble single-centre atomic orbitals. La Paglia (10) has shown that the electronic wavefunction of the first members of the Rydberg series may be described by a molecular orbital which is located at a single centre (united atom approximation) providing the principle quantum number is set at n = 3. This is the procedure adopted here; it is to be contrasted with the recent RCNDO calculations of Salahub and Sandorfy (11), who constructed a set of Rydberg MO's as a linear combination of atomic Rydberg orbitals summed over all of the nuclear centres.

Mulliken (12) has developed a simple technique which allows one to calculate the Slater orbital exponent ζ for united atom atomic orbitals of the type used here. In his method, the position of the maximum radial density of the outermost loop of a Rydberg AO is given by:

$$r_{max} = \frac{a_o n^{*2}}{Z}$$

In this formula a_o is 0.529 Å, the radius of the n = 1 orbit of the hydrogen atom according to the Bohr theory, Z is the charge on the atomic core in units of the electron charge, and n* is the effective principal quantum number. With Z = 1 for a neutral molecule, and n* = 3 according to La Paglia's results, we obtain r_{max} = 4.8 Å (9.07 a.u.). For Slater type orbitals with n = 3, the radial function is

$$R_3(r) = (2\zeta)^{7/2}[(2n)!]^{-1/2} r^2 \exp(-\zeta r)$$

A plot of the radial charge density, defined as $4\pi r^2 R^2 dr$, versus r has a maximum whose position gives the most probable value for r. At this point

$$0 = \frac{d}{dr}(4\pi r^2 R^2) = \frac{2\zeta^{7/2}}{((2n)!)^{1/2}} \cdot 4\pi \frac{d}{dr}(r^6 \exp(-2\zeta r))$$

i.e.,

$$6r^5 \exp(-2\zeta r) - 2\zeta r^6 \exp(-2\zeta r) = 0$$

$$3 - \zeta r = 0$$

As a result, $\zeta = 0.33\ (\text{a.u.})^{-1}$

The critical parameter in the CNDO scheme which determines the energy of the Rydberg orbitals is the Mulliken electronegativity, χ, which is defined as the sum of the ionization potential and the electron affinity divided by two. In the pure united atom approximation, χ is a direct measure of the energy of the one-electron Rydberg state relative to the corresponding ionization potential. In this case, χ can be directly related to I_μ and is given by the spectroscopic Rydberg term value. This is the procedure which was employed by

Sandorfy(11). According to Betts and McKoy's most recent calculations on formaldehyde (13), the χ parameter for the 3s, 3p and 3d terms is 3.67, 2.59, and 2.25 ev respectively.

The remaining parameter β_{AB}, which describes the overlap density between centres A and B, is the empirical parameter which was adjusted by PSS to give the best fit of their eigenvector coefficients to accurate ab initio calculations using the same basis set. In order to reduce the overlap between valence and Rydberg orbitals, it has been found (11) that β_{AB} must be at least an order of magnitude smaller for Rydberg orbitals than for the corresponding valence orbitals. After some adjustment, a value of 0.71 for β was found to be acceptable for the n = 3 Rydberg orbitals of formaldehyde.

In these calculations, the 3s, 3p and 3d Rydberg orbitals were centred at a point 0.5 Å from the carbon atom, on the carbonyl axis. This choice is not critical since Buenker and Peyerimhoff (14) in their exhaustive ab initio calculations located their Rydberg orbital on the carbon while Whitten and Hackmeyer (15) in their calculations elected to centre their Rydberg on the oxygen atom, and the two sets of results are in good agreement. This is not too surprising when it is recognized that the 9.1 Å diameter of the Rydberg orbital exceeds the molecular diameter of the formaldehyde core by a factor of four.

These modifications of the program are sufficient to completely specify the additional molecular orbitals required for our calculations. The purpose of this exercise was not to optimize the CNDO parameters, but to obtain estimates of the molecular structures of the molecule in its various Rydberg excited states. For this reason, we did not attempt to match the transition energies precisely to the experimental

values by refining these empirical parameters further.

(C) CNDO Modifications---Parent Configuration Molecular Orbitals

Although the Mulliken overlap population calculation[1] provides information about the changes in geometrical structure on excitation, the results are qualitative rather than quantitative. For more precise information, it is necessary to examine the nature of the potential functions which control the symmetric vibrations of formaldehyde in its various electronic configurations. This establishes not only R_e, the equilibrium values for the three structural co-ordinates in each of the electronic states, but also the harmonic force constant K_e, and is sufficient to completely define the dynamics of the molecule in each of its excited states.

Kroto and Santry (17) have shown that the virtual orbital treatment (an MO calculation which is self-consistent with respect to the ground state configuration) is not suitable for the evaluation of K_e and R_e. They suggest that the calculation be done by a procedure which is self-consistent with respect to the particular electronic configuration under consideration. Recently, this idea has been employed in the superb ab initio calculations of Peyerimhoff and Buenker (8, 14); their method is referred to as PCMO-CI (parent configuration molecular orbital with configuration interaction). Their results, which are listed in Table 4, justify this use.

In order to follow their example and introduce a PCMO modification into the CNDO/2 program, it was necessary to redesign the manner in which the orbital density was calculated and to control the initial electronic configuration. To make the task easier and less confusing, we first ordered the columns of the eigenvector matrix into the three blocks which correspond to the three representations A_1, B_1, and B_2

[1] see Appendix A

Table 4

Comparison of the Observed and Calculated Transition Energies for the Extravalence States of Formaldehyde (ev.)

	ref.15	ref.14	ref.31	CNDO/2*	Exp't†
$^1B_2(n,3s)$	7.48	7.38	7.14	7.22	7.08
$^1A_1(n,3p_y)$	8.30	8.11	8.41	8.30	7.97
$^1B_2(n,3p_z)$		8.39	7.98	8.34	8.14
$^1A_2(n,3p_x)$		9.07	8.63	8.63	
$^1B_2(n,4s)$			9.33		9.27
$^1B_2(n,3d_z2)$			9.44		
$^1B_1(n,3d_{xy})$			9.45		
$^1B_2(n,3d_{x^2-y^2})$			9.46		
$^1B_2(n,4p_z)$			9.71		9.63

*Results from this work.

†See ref. 34.

of the C_{2v} point group (without d orbitals, there are no elements of A_2 symmetry). Within each block, the columns were arranged in order of ascending electronic energy. The density matrices were then calculated in the usual manner, but the molecular orbitals used were specified according to the electron configuration of the appropriate electronic state. In this way, it was possible to calculate potential functions which were self-consistent with respect to the electronic configuration which generated them. The next consideration then is the calculation of K_e and R_e for each symmetric potential.

(D) Calculation of CNDO Equilibrium Force Constants and Structures

In a diatomic molecule, there is only one internuclear co-ordinate and consequently there is no question of the correct independent variable (structural parameter) to be used. That is, a plot of total energy (electronic plus nuclear) against increasing bond length produces a one-dimensional potential function which yields equilibrium values for K_e and R_e as well as a dissociation limit.

For a polyatomic molecule, the calculation can become multi-dimensional and difficult to solve. One standard procedure, however, is to use the Wilson's **F** and **G** matrix formalism (18). A set of internal parameters ΔR, $\Delta\theta$, $\Delta R\Delta\theta$, ..., etc. is constructed to represent stretching or bending displacements along the bonds or perpendicular to them. The force constants derived for these co-ordinates are the general valence force field constants which form the Wilson's **F** matrix. This information is coupled with the **G** matrix through the relationship

$$\mathbf{FGL} = \mathbf{L}\Lambda$$

and will yield the harmonic frequencies λ_i and the **L** matrix which relates the internal co-ordinates ΔR_i to the normal co-ordinates ΔQ_i:

$$\mathbf{R} = \mathbf{LQ}$$

H_2CO has three symmetric modes of vibration, as shown in Figure 1, and it was only these three with which we worked. Correspondingly, we selected three co-ordinates, ΔR_{CO}, ΔR_{CH}, and $\Delta\alpha_{HCH}$, and varied these to obtain the minimum energy with respect to each co-ordinate. We assumed that all three were independent and did not attempt to adjust them simultaneously. Rather, two co-ordinates were maintained at their ground state values while the third was varied systematically.

When we had established three points near the minimum of the potential well, we calculated the harmonic force constants K_e, and equilibrium values for R_e. The reference frame was changed to symmetry co-ordinates by the following transformations:

$$S_{CO} = \Delta R_{CO}$$

$$S_{CH} = \frac{1}{\sqrt{2}}(\Delta R_{CH_1} + \Delta R_{CH_2})$$

$$= \sqrt{2}\,\Delta R_{CH}$$

$$S_{HCH} = \frac{1}{\sqrt{6}}(\Delta\beta_{H_1CO} + \Delta\beta_{H_2CO} - 2\Delta\alpha_{HCH})$$

$$= \frac{-3}{\sqrt{6}}\Delta\alpha_{HCH}$$

The CNDO/2 ground state force constants were then adjusted to the experimental results given by Shimanouchi (19) and the excited state constants multiplied by the same scaling factor. The off-diagonal elements, which were not calculated with our technique, were taken directly from the experimental data, and did not change with the electronic state.

With the rescaled set of excited and ground state F matrices and the equilibrium ground state geometry given by Takagi and Oka (3), it is possible to obtain the symmetric vibrational frequencies for each ionic state. However, in order to calculate band intensities and to reproduce an experimental intensity pattern, we must make use of the concepts embodied in the Franck-Condon principle (20).

(E) The Franck-Condon Principle

In general, the excited state geometry for a polyatomic molecule differs from that of the ground state. The ground state geometry can often be experimentally determined or estimated by analogy, but structures are known for only a few excited states. The Franck-Condon principle (21a-c) offers a method of obtaining this information if resolvable rotational fine structure cannot be determined as is the case in the present study. According to this principle, the relative intensities of the vibrational bands of an electronic absorption or ionic system depend on the changes in the geometrical structure on electronic excitation. The vibrational transitions which have the greatest probability are those for which there is no geometry change, i.e., the transitions which occur completely vertically. The bands of a transition form a pattern of increasing intensity from the origin to the maximum and then decrease again. From this pattern, the shift of the excited state potential function relative to the ground state function can be theoretically determined for each symmetric normal mode which is active in the spectrum. This method is applicable to any electronic transition for which both electronic states have structures of the same symmetry. Necessary information includes the geometrical structure and the totally symmetric frequencies of the ground state, as well as the vibrational analysis of a vibronic band system and the resulting information about the totally symmetric frequencies of the excited state. The relative intensities of a few selected vibronic bands must be measured for the following calculation, which has been developed in detail by Coon, de Wames, and Loyd (20).

Two absorption bands, a and b, which are temperature insensitive, are selected so that their vibrational assignments differ by only the

i^{th} symmetric mode of the excited state. Let ε_a and ε_b be their respective peak molar extinction coefficients, and their frequencies be σ_a and σ_b. Since the absorption intensity is proportional to the square of the dipole moment, it can be shown that

$$\frac{\varepsilon_a/\sigma_a}{\varepsilon_b/\sigma_b} = \left[\frac{R_i(\nu_{ia},0)}{R_i(\nu_{ib},0)}\right]^2$$

where $R_i(\nu_i',\nu_i'')$ is the overlap integral of two harmonic oscillator wave functions with centres at different points along the Q (normal co-ordinate) axis. This integral has been expressed by Ansbacher (22); some useful ratios of the integral follow from his formula:

$$\frac{R(1,0)}{R(0,0)} = \frac{\sqrt{2}\,\beta^2\gamma}{1+\beta^2}, \quad \text{where } \beta_i^2 = \frac{\nu_i''}{\nu_i'}$$

$$\gamma_i = -\left(\frac{4\pi^2 c\nu_i'}{h}\right)^{1/2} d_i$$

$$\frac{R(2,0)}{R(0,0)} = \frac{1}{\sqrt{2}\,(1+\beta^2)}\left[\frac{2\beta^4\gamma^2}{(1+\beta^2)} + (1-\beta^2)\right]$$

$$\frac{R(3,0)}{R(0,0)} = \frac{\beta^2\gamma}{\sqrt{3}\,(1+\beta^2)^2}\left[\frac{2\beta^4\gamma^2}{(1+\beta^2)} + 3(1-\beta^2)\right]$$

For a first approximation, d_i is related to the change in internal co-ordinates R_i by the relation

$$R'' = L''D$$

Since the sign of each element in the column matrix D is undetermined, there are 2^s (where s is the number of symmetric modes) excited state models consistent with the observed intensities. The choice of one model over the others may be based on theoretical considerations or on experimental information from an analysis of the band envelope.

On the other hand, if an estimate of the excited state structure and the symmetric frequencies are available, it is possible to reverse the procedure and calculate an intensity pattern. This method can prove very useful if the assignment of the spectrum is in doubt, or if the intensities are low and the geometry changes small. It must be realized, however, that the above expressions account for only the first three quanta of a series relative to a reference band, usually the origin band.

Chapter 3

The experimental data used in this work was obtained from three separate sources--the photoelectron spectra (23), inelastic scattering experiments (24,25), and the vacuum ultraviolet spectra. We shall briefly discuss these techniques and the information which can be taken from each.

(A) Photoelectron Spectroscopy

Photons in the vacuum ultraviolet region of the spectrum, with an energy of about 10 ev, may interact with atomic or molecular gases and provide sufficient energy to completely ionize the molecule. The process which we are concerned with is

$$M \longrightarrow M^+ + e^- \text{ (direct ionization)}$$

and the electron which is removed is not necessarily the outermost electron, but depends on the energy supplied. Because the process of ionization, or the loss of an electron, may be regarded as the first step in an intravalence or Rydberg transition, the analysis of the photoelectron spectrum can provide vital clues about frequency and structural changes in the excited state.

The photoelectron spectra of formaldehyde and its deuterium analog D_2CO were presented in detail by Baker, Baker, Brundle, and Turner (23), and the former is reproduced in Figure 4. The authors used a high-resolution photoelectron spectrometer which is described by Turner (26). They have isolated four separate transitions and assign these respectively as $^2B_2(n) \leftarrow \tilde{X}^1A_1$, $^2B_1(\pi) \leftarrow \tilde{X}^1A_1$, $^2B_2(\sigma_{CH}) \leftarrow \tilde{X}^1A_1$, and $^2A_1(n\sigma) \leftarrow \tilde{X}^1A_1$. All four exhibit vibrational activity, and the frequency assignments given by the authors are listed in Table 5.

Figure 4

Photoelectron Spectrum of H_2CO (ref.23)

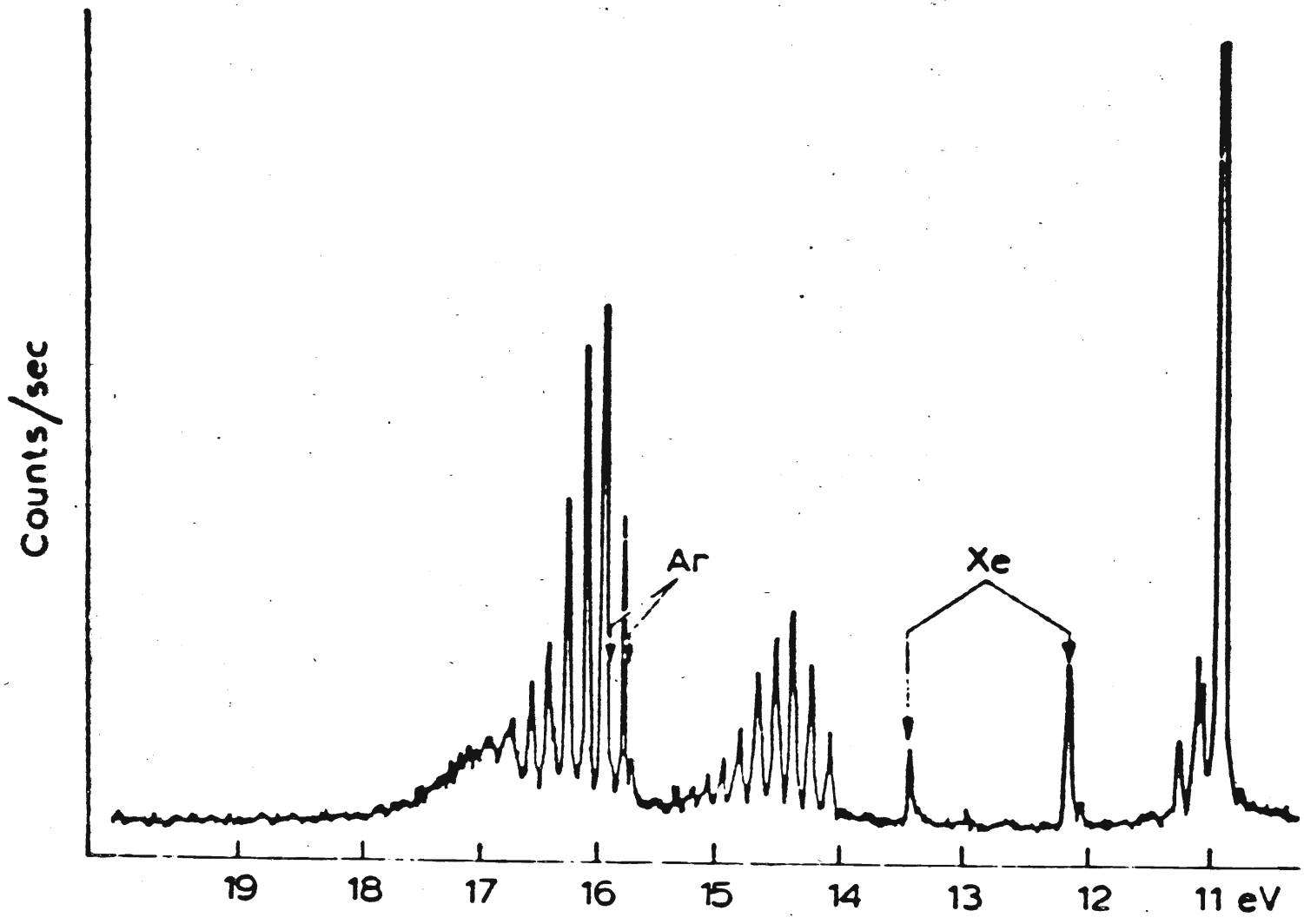
Counts/sec
Ar
Xe
19
18
17
16
15
14
13
12
11 eV

Table 5

Calculated and Observed Vibrational Frequencies for the Ionic States of Formaldehyde ($\pm$ 50 cm^{-1})

		CNDO/2		Franck-Condon		ref. 27	
		H_2CO	D_2CO	H_2CO	D_2CO	H_2CO	D_2CO
$\tilde{X}^1A_1$ State	ν_1	2782.9	2047.7	2782.9	2047.7	2766.4	2055.8
	ν_2	1747.7	1690.4	1747.7	1690.4	1746.1	1700
	ν_3	1506.6	1094.1	1506.6	1094.1	1500.6	1105.7
$^2B_2$ State	ν_1	2671	1946	2574	1878	2560	1910
	ν_2	1584	1557	1583	1554	1590	1560
	ν_3	1242	896	1205	869	1210	870
$^2B_1$ State	ν_1	2697	1961	2727	1971	--	--
	ν_2	1415	1471	1211	1212	1210	1210
	ν_3	1521	1041	1385	990	1400	960
$^2A_1$ State	ν_1	2668	1946	2726	1969	--	--
	ν_2	1588	1556	1269	1269	1270	1270
	ν_3	1369	990	1295	926	1270	935

(B) Inelastic Electron Scattering

The procedure for this technique is similar to that for photo-ionization except that the interaction is between a low-energy electron and a molecule. The effect of this bombardment is excitation rather than ionization, but the relative intensities of the transitions are a function of the scattering angle (25), and generally spin forbidden transitions are favoured only at large scattering angles.

The electron scattering spectrum of formaldehyde has been determined in the energy loss range between 0 and 16.0 ev by Weiss, Kuyatt, and Mielczarek (24), and is reproduced in Figure 5. Three Rydberg series can be identified in the region 7-11 ev which correlate with ns, np, and nd Rydberg configurations leading to the n ionization limit. Beyond 11 ev, two other series converging to separate ionization limits are observed and tentatively linked with the $^2B_1(\pi)$ and $^2A_1(n\sigma)$ photoelectron configurations.

Figure 5

Inelastic Electron Scattering Spectrum of Formaldehyde (ref.24)

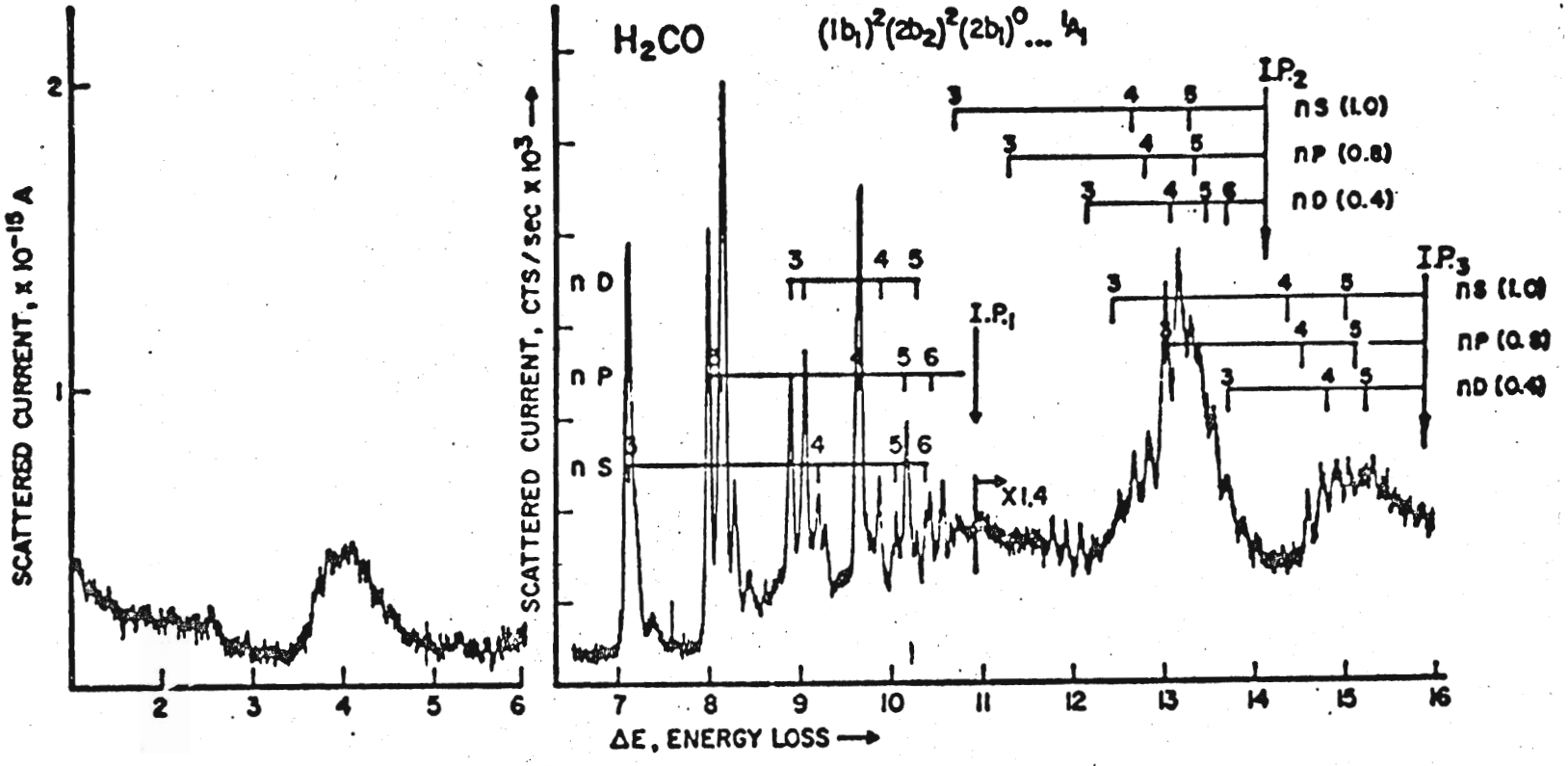
H2CO
(1b1)2(2b2)2(2b1)0 ... 1A1
I.P.2
nS (1.0)
nP (0.8)
nD (0.4)
I.P.3
nS (1.0)
nP (0.8)
nD (0.4)
I.P.1
nD
nP
nS
X1.4
SCATTERED CURRENT, x 10-15 A
SCATTERED CURRENT, CTS/sec x 10-3
ΔE, ENERGY LOSS

(C) Ultraviolet Absorption Spectroscopy

The source of the continuous radiation used here is high-frequency light emission, usually Xe, Kr, Ar, or H_2 continua excited by microwave discharge. These are comparatively low energy sources and span the following spectral regions: H_2, 3400-1800 Å; Xe, 2200-1500 Å; Kr, 1600-1300 Å; Ar, 1400-1200 Å. Impurities in the light source are a problem here which may be partially eliminated by the addition of getters. Also the impurity atomic lines are useful internal frequency standards. The spectrum is linear with wavelength rather than energy and is generally recorded photographically rather than electronically.

The spectra used in this thesis were recorded by Moule and Bell (46) on a McPherson 3 meter concave grating spectrograph which was operated in the first order. With an 1100 line/mm. grating, the plate dispersion in this region was 2.7 Å/mm. The spectra were calibrated when possible by a least squares fit of the absorption features to a dispersion relationship which was obtained from the known frequencies of the prominent impurity lines. Because of the inherent diffuseness of some of the bands, it was necessary to take measurements from either the prints or the microdensitometer traces of the spectra. The samples of formaldehyde, D_2CO, $D_2C^{13}O$ and HDCO were obtained from Merck, Sharpe, and Dohme in the form of solid paraformaldehyde. To liberate the monomer, a small amount of the paraformaldehyde was placed in a sidearm which was attached directly to the absorption cell. This was then warmed with a Bunsen burner to about 100°C. The pressure of the vapour was recorded with a Pirani gauge. In all of these experiments, the path length of the absorption cell was fixed at 10 cm. and the pressure varied in incremental steps. Some difficulty was encountered in the formation of a white solid polymer on the MgF_2 windows of the

cell, and it was necessary to periodically dismantle and clean the exterior optical train. The slit width varied over the range 10-40 μ depending on the spectral region. In most instances, 1/2 to 1 hour exposures were required to provide sufficient plate blackening. Prints were developed on high-contrast Ilford paper for maximum definition. The spectra for the four isotopes over the three spectral regions are shown in Figure 6.

Figure 6

Ultraviolet Spectra of H_2CO, HDCO, D_2CO, and $D_2C^{13}O$

(a) Region from 1800 Å to 1560 Å

(b) Region from 1560 Å to 1329 Å

(c) Region from 1380 Å to 1215 Å

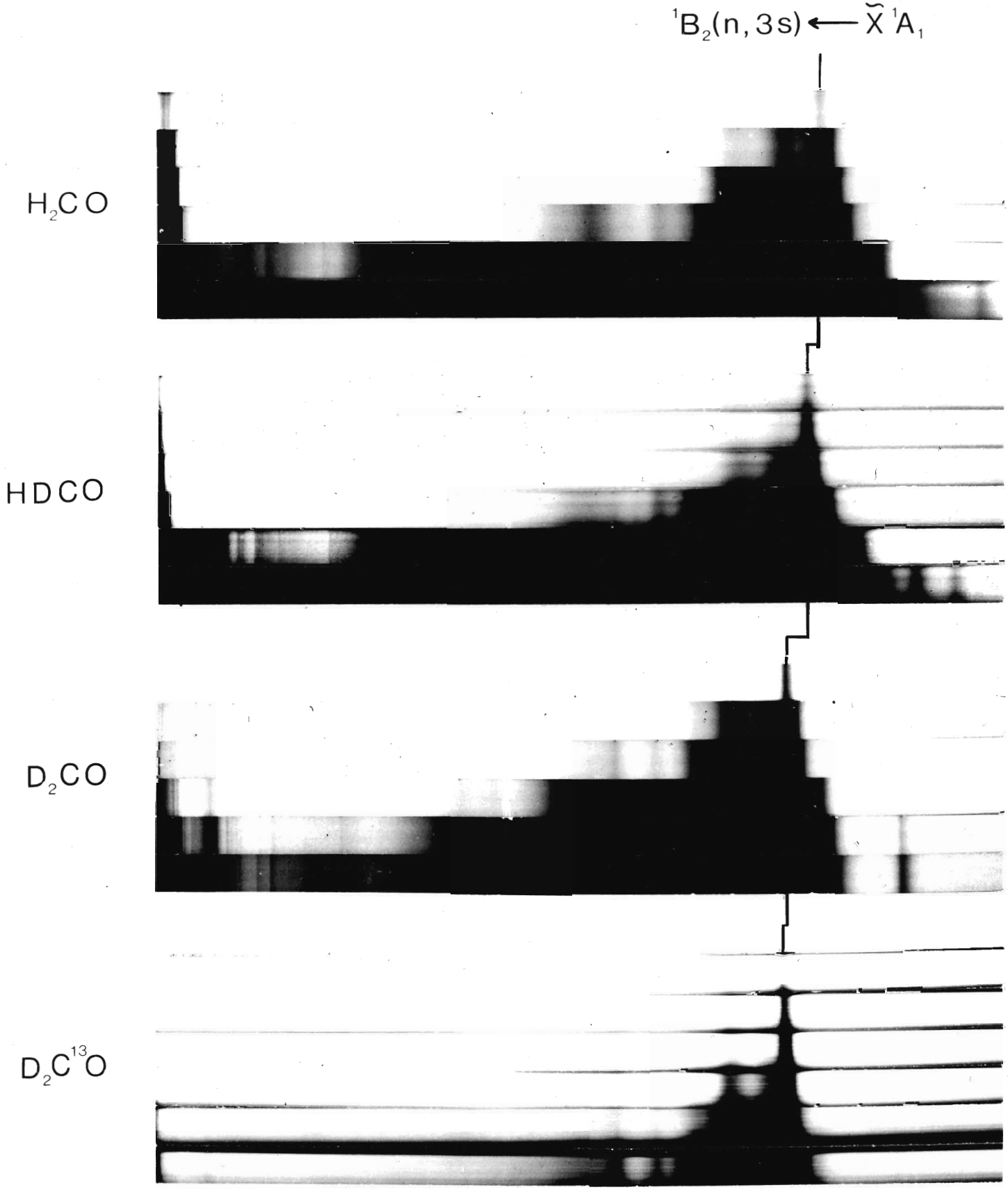
$^1B_2(n,3s) \leftarrow \tilde{X}\,^1A_1$
H_2CO
$HDCO$
D_2CO
$D_2C^{13}O$

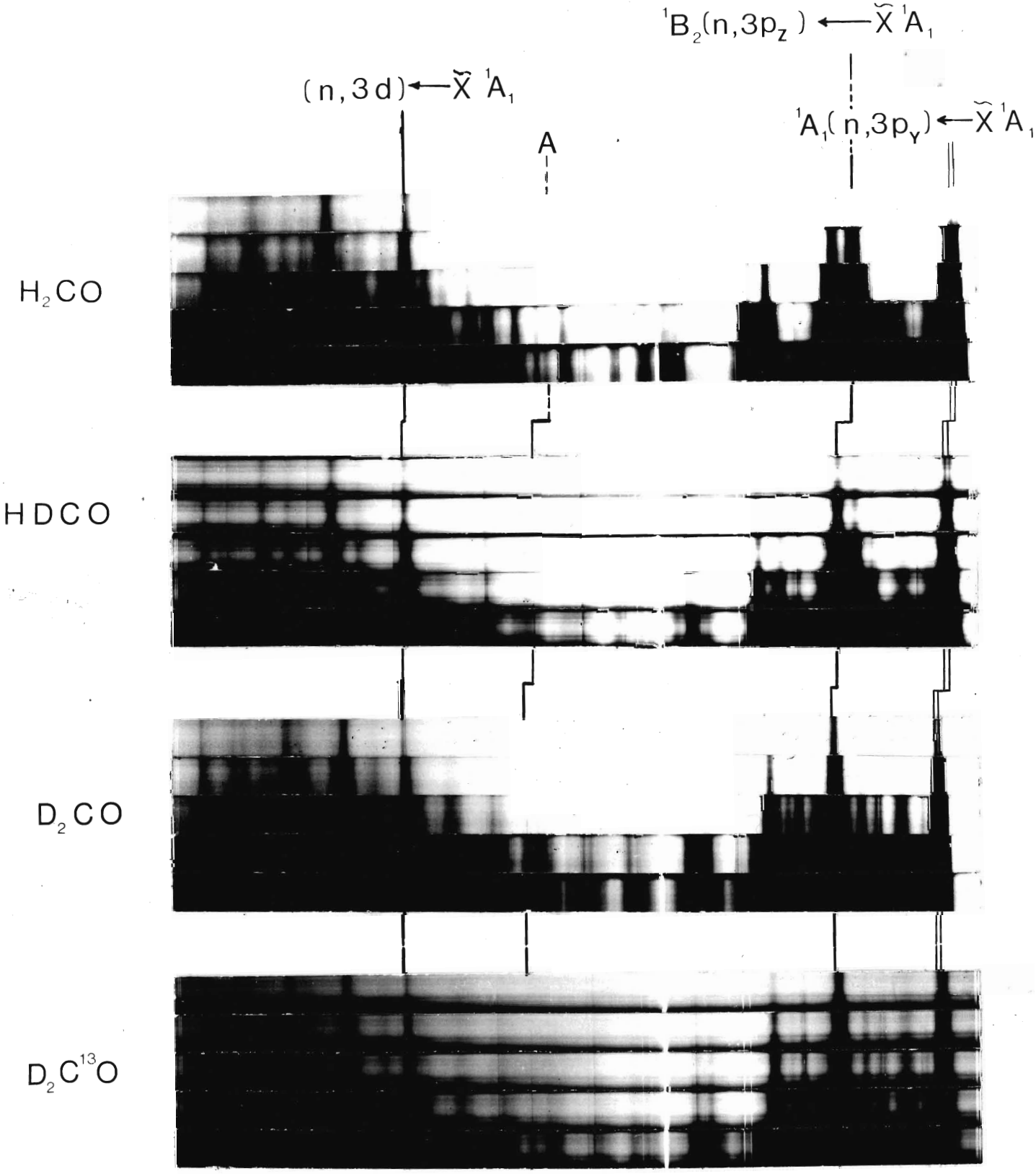
$^1B_2(n,3p_z) \leftarrow \tilde{X}\ ^1A_1$
$(n,3d) \leftarrow \tilde{X}\ ^1A_1$
$^1A_1(n,3p_Y) \leftarrow \tilde{X}\ ^1A_1$
A
H_2CO
HDCO
D_2CO
$D_2C^{13}O$

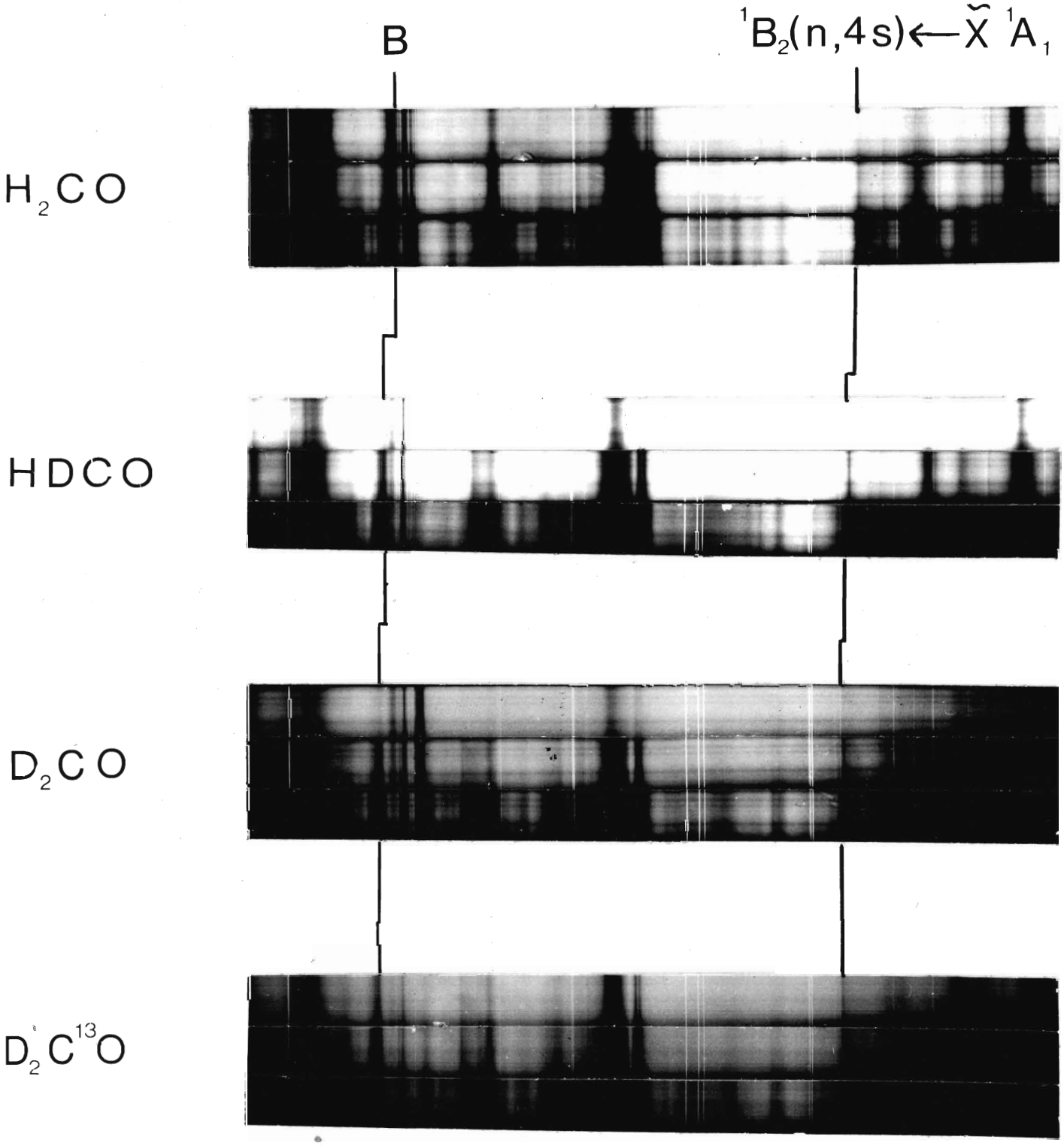
B
$^1B_2(n,4s)\leftarrow\tilde{X}\ ^1A_1$
H_2CO
HDCO
D_2CO
$D_2C^{13}O$

Chapter 4

Ionic States

A number of results can be derived from the above calculations concerning the ionic, Rydberg, and intravalence transitions in formaldehyde. Using the Franck-Condon principle, it is possible to generate a theoretical band contour to correlate closely with the experimental spectrum for the photoelectron states. This in turn produces excited state geometries and frequencies which may be used as a first approximation for related Rydberg states. In addition, the vibrational structure of a number of Rydberg transitions which appear in the vacuum ultraviolet can be assigned with some degree of certainty, and this is a vital aid in establishing the upper state electronic configuration and hence the electronic transition. Each state has its own characteristics and we shall therefore discuss the results under the separate headings of ionic, valence or Rydberg states.

(A) $^2B_2(n)$ State

It has been generally accepted that the lowest-lying ionic state of formaldehyde results from the removal of an electron from a non-bonding orbital centred on the oxygen and that there should be very little change in the equilibrium molecular structure on excitation. A preliminary survey of the spectrum, Figure 4, indicates that the gross vibronic structure is compatible with this idea; that is, the origin band has an intensity of 100 while the single quantum additions have an intensity of 5 to 10. Turner (24) was able to assign the three bands which appear to higher frequencies from the origin to the three a_1 modes in both H_2CO and D_2CO. His assignments for the two

isotopes H_2CO/D_2CO are: ν_1 = 2560/1910; ν_2 = 1590/1560; ν_3 = 1210/870. These values are to be compared to the $\tilde{X}$ values of ν_1 = 2780/2056; ν_2 = 1744/1700; ν_3 = 1503/1106. It is apparent that quite large changes occur in ν_3 on excitation; i.e., for H_2CO, ν_3'/ν_3'' = 0.80 and for D_2CO, ν_3'/ν_3'' = 0.79, and this is not entirely compatible with the intensity of $3_o^1(H_2CO)$, which is 5.4 relative to an intensity of 100 for the 0-0 band. The anomalies in the intensity distribution and the frequency shifts suggest that the spectroscopic analysis of this transition is more complicated than Turner had envisaged. With this in mind, we performed PCMO LCAO-MO calculations on the $\tilde{X}$ and $^2B_2$ states of formaldehyde in which the three totally symmetric structural parameters R_{CH}, R_{CO}, and α_{HCH} were varied systematically and the total energy evaluated. The results of a three-point interpolation of this data are the force constants and the equilibrium bond distances and angles, which are listed in Table 6. Here again we notice the large change in HCH angle on excitation, where the $\tilde{X}$ CNDO/2 value is calculated to be 114.2° which is in excellent agreement with Oka's microwave value of 116° 31', while the $^2B_2$ value is 120.0° which represents an increase of 5.8° on excitation. While it is now well-recognized that CNDO is incapable of yielding satisfactory values for stretching force constants and bond lengths, it does provide bond angles and angle bending force constants which are consistent with the best ab initio results. The change in bond angle predicted by CNDO consequently is much larger than one would anticipate from a simple Franck-Condon one-dimensional analysis of the spectrum. For example, when we employed the calculated parameters ΔR_{CO} = 0.0072 Å, ΔR_{CH} = 0.0092 Å and $\Delta\alpha_{HCH}$ = 5.8°, and Turner's frequency assignment,

Table 6

(a) Calculated Geometry Changes for the Ionic States of Formaldehyde

(b) Symmetrized and Normalized Force Constants for the Ground and Ionic States of Formaldehyde (mdyne/Å and mdyne Å)

		(a)			(b)		
		ΔR_{CH} (Å)	ΔR_{CO} (Å)	$\Delta\alpha_{HCH}$ (°)	K_{CH}	K_{CO}	K_{HCH}
$\tilde{X}^1A_1$ State	ref. 19				4.42	12.68	0.56
	CNDO/2	1.16	1.25	114.2	11.91	33.93	0.63
	CNDO/2 (normalized)				4.40	12.76	0.56
$^2B_2$ State	CNDO/2	0.0095	0.0072	5.8	11.02	28.97	0.42
	CNDO/2 (normalized)				4.07	10.90	0.38
	Franck-Condon	0.015 ±0.003	-0.020 ±0.005	5.0 ±0.4	3.78	10.90	0.29
$^2B_1$ State	CNDO/2	0.008	0.083	4.3	11.22	25.42	0.57
	CNDO/2 (normalized)				4.15	9.56	0.51
	Franck-Condon	0.008 ±0.003	0.130 ±0.010	1.0 ±0.4	4.25	6.60	0.41
$^2A_1$ State	CNDO/2	0.008	0.017	13.8	10.98	28.73	0.51
	CNDO/2 (normalized)				4.06	10.80	0.46
	Franck-Condon	0.008 ±0.003	0.080 ±0.005	14.0 ±0.7	4.24	7.28	0.32

we obtained for H_2CO the intensities $1_o^1 = 0.34$, $2_o^1 = 0.24$ and $3_o^1 = 34.0$ relative to $0_o^\circ = 100$. These can be compared to the corresponding observed data $1_o^1 = 2.5$, $2_o^1 = 6.2$ and $3_o^1 = 5.6$. This large change in angle is not altogether unexpected since ν_3 changes by 20% on ionization and the normal co-ordinates for the $^2B_2(n)$ state are expected to be quite different from the ground state. In order to correlate the intensity with the geometry, it is necessary to take account of the differences in internal mixing in the two combining states. Coon, de Wames, and Loyd (20) have constructed a multi-dimensional formula which does take this into account. This method is described in section E of the theory. In our case, we use the excellent set of F matrix elements which have been evaluated for the $\tilde{X}$ state by Shimanouchi (19), and a set of d's which were obtained initially from the structural changes evaluated with our CNDO/2 program. The Coon method, under these approximations, did yield a relatively satisfactory fit to the observed data with the three modes for H_2CO calculated at $1_o^1 = 1.9$, $2_o^1 = 1.1$ and $3_o^1 = 19.0$. At this stage of the analysis the d parameters were systematically refined to obtain a fit to the data. However, a fundamental inconsistency was found in the intensity data for H_2CO and D_2CO in that the 3_o^1 band in the two isotopes could not be uniquely fitted. A closer examination of the molecular orbital representation for the n orbital, shown in Figure 2, provides the clue to solving this problem, since it indicates that the n orbital is anti-bonding in the CO bond. This is substantiated by the molecular orbital coefficients for the $n(b_2)$ MO, for which we have:

$$\psi_n = 0.3012\phi_{p_y(C)} - 0.7616\phi_{p_y(O)} + 0.4057\phi_{s(H_1)} - 0.4057\phi_{s(H_2)}$$

That is, the nominally non-bonding orbital, ψ_n, is in fact anti-bonding in the carbonyl bond ($\phi_{p_y}(C)$ and $\phi_{p_y}(O)$ appear in the linear combination with opposite signs) and hence the removal of an electron from this orbital should lead to structural stability in the $^2B_2(n)$ ionization state and to the reduction in CO bond length. From Table 6 the equilibrium values for $\tilde{X}^1A_1$ and $^2B_2$ states are calculated to be 1.250 and 1.257 $\mathring{A}$ respectively. The potential functions in this instance show that the CO bond length increases on ionization which is contrary to our expectations. To resolve this problem, we performed the Mulliken overlap population analysis which is shown in Table 7. Here the foregoing question is clarified, since the C=O overlap population for the n orbital in the $\tilde{X}$ state is -0.0997, while in the $^2B_2(n)$ state it is - 0.0770. We therefore conclude that the sign of R_{CO} was incorrectly introduced into the Franck-Condon calculations and that the CO bond decreases in length on ionization. This change in internal co-ordinates is related to the change in normal co-ordinates through the relationship

$$\mathbf{D} = \mathbf{L}^{-1}\mathbf{S} \quad \text{or} \quad \Delta\mathbf{D} = \mathbf{L}^{-1}\Delta\mathbf{S}$$

In particular, for H_2CO we have

$$\Delta d_3 = L_{31}^{-1}\Delta S_1 + L_{32}^{-1}\Delta S_2 + L_{33}^{-1}\Delta S_3$$

$$= (0.0162)(0.0130) + (-0.0827)(-0.0072) + (0.0725)(-0.1383)$$

The second and third terms in this expansion are considerably larger than the first term, and are of opposite sign to each other. The result is that while the 5° change in α_{HCH} makes a substantial contribution to Δd_3, it is in the reverse direction to and is partially cancelled by the structural changes in R_{CO} and R_{CH}. For D_2CO,

Table 7

Mulliken Overlap Population for the Ground State and the $^2B_2$, $^2B_1$, and $^2A_1$ Ionic States

Molecular Orbitals \ Bond		Ground state				$^2B_2$ state			
		CO	CH	OH	HH	CO	CH	OH	HH
A_1	σ_{CO}	0.5854	0.0476	0.0206	0.0062	0.5800	0.0371	0.0179	0.0044
	σ_{CH}	0.0462	0.2972	-.0106	0.0496	-.0017	0.2648	-.0040	0.0389
	$n\sigma$	0.0564	0.0456	-.0124	0.0128	0.0998	0.0824	-.0159	0.0164
	σ^*_{CH}	-.0770	-.3834	0.0172	0.0822	-.0578	-.3573	0.0176	0.0852
	σ^*_{CO}	-.4516	-.0072	-.0146	0.0036	-.5879	-.0211	-.0203	0.0084
B_1	π	0.2165	--	--	--	0.1950	--	--	--
	π^*	-.2163	--	--	--	-.1968	--	--	--
B_2	σ_{CH}	0.0823	0.0889	0.0080	-.0192	0.1545	0.1847	0.0134	-.0354
	n	-.0997	0.0972	-.0232	-.0504	-.0770	0.0815	-.0226	-.0484
	σ^*_{CH}	-.0661	-.2752	0.0070	-.0056	-.0798	-.2660	-.0093	-.0708

Molecular Orbitals \ Bond		$^2B_1$ state				$^2A_1$ state			
		CO	CH	OH	HH	CO	CH	OH	HH
A_1	σ_{CO}	0.5851	0.0381	0.0178	0.0022	0.5737	0.0396	0.0186	0.0047
	σ_{CH}	-.0031	0.2685	-.0049	0.0388	-.0056	0.2957	-.0104	0.0484
	$n\sigma$	0.0996	0.0763	-.0149	0.0151	0.0729	0.0457	-.0107	0.0119
	σ^*_{CH}	-.0876	-.3629	0.0224	0.0881	-.0674	-.3667	0.0200	0.0885
	σ^*_{CO}	-.5920	-.0199	-.0205	0.0082	-.5878	-.0142	-.0175	0.0061
B_1	π	0.2098	--	--	--	0.1960	--	--	--
	π^*	-.2098	--	--	--	-.1960	--	--	--
B_2	σ_{CH}	0.1824	0.1377	0.0137	-.0247	0.1826	0.1332	0.0148	-.0239
	n	-.1381	0.1437	-.0206	-.0476	-.1387	0.1485	-.0205	-.0487
	σ^*_{CH}	-.0443	-.2814	0.0058	-.0824	-.0439	-.2816	0.0057	-.0821

$$\Delta d_3 = (0.0298)(0.0130) + (-0.1071)(-0.0072) + (0.1001)(-0.1383)$$

and since $L_{33}^{-1}(H_2CO)$ is less than $L_{33}^{-1}(D_2CO)$ it follows that the destructive interference among R_{CO}, R_{CH} and α_{HCH} is less complete, and hence 3_o^1 has 60% more intensity in D_2CO than it has in H_2CO. This analysis then shows that the quite large changes which were computed by the CNDO techniques are completely compatible with the Franck-Condon intensity profile. That is, by judiciously selecting the sign of the internal co-ordinate change, it is possible to construct a spectrum in which very little Franck-Condon activity appears in the ν_3 normal co-ordinate even though the change in HCH angle is given an appreciable size.

Spectroscopic parameters were refined by fitting a calculated photoelectron band profile to Turner's experimental data. The calculated profile was obtained using the three diagonal force constants K_{11}, K_{22} and K_{33} and the three structural parameters R_{CO}, R_{CH}, and α_{HCH} as variables. The frequencies for the excited state were calculated by the Wilson's **F** and **G** matrix method (18) in which the off-diagonal force constant matrix elements were transferred from the ground state, and the **G** matrix elements were fixed at their ground state values. Intensity distribution was obtained for the progression sequence and cross-sequence bands for the v' ranging from 1 to 3 by the Coon method. Frequencies and intensities were plotted using a graph plotter in which the photoelectron lines were broadened by a Lorentzian distribution to a half-width of 32 mev. This is to be compared to Turner's spectroscopic resolution of 30 mev. The best simultaneous fit to the H_2CO and D_2CO data was obtained for the parameters which are quoted in Table 6. The resulting theoretical spectrum is shown in Figure 7.

Figure 7

Comparison of Theoretical and Experimental Results for the $^2B_2(n)$ Ionic State

(a) H_2CO (i) Franck-Condon calculation

(ii) experimental (ref. 27)

(b) D_2CO (i) Franck-Condon calculation

(ii) experimental (ref. 27)

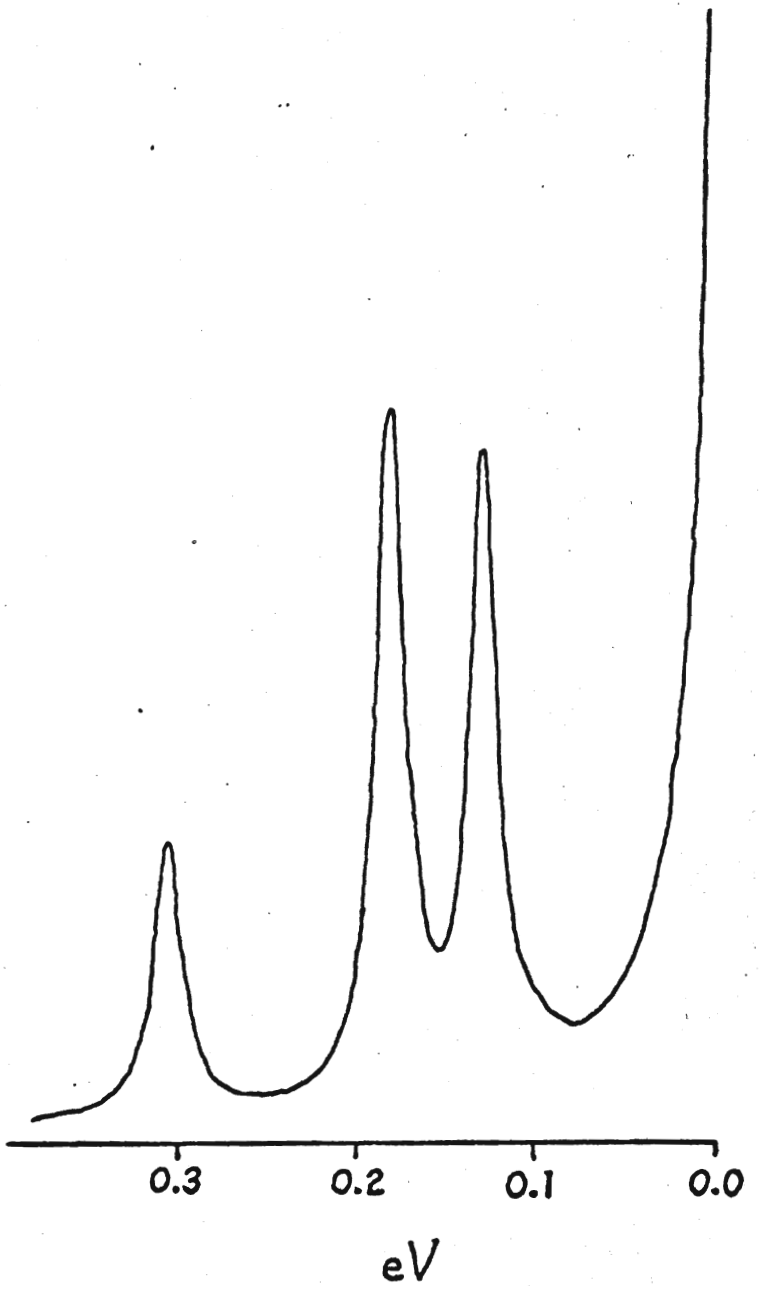

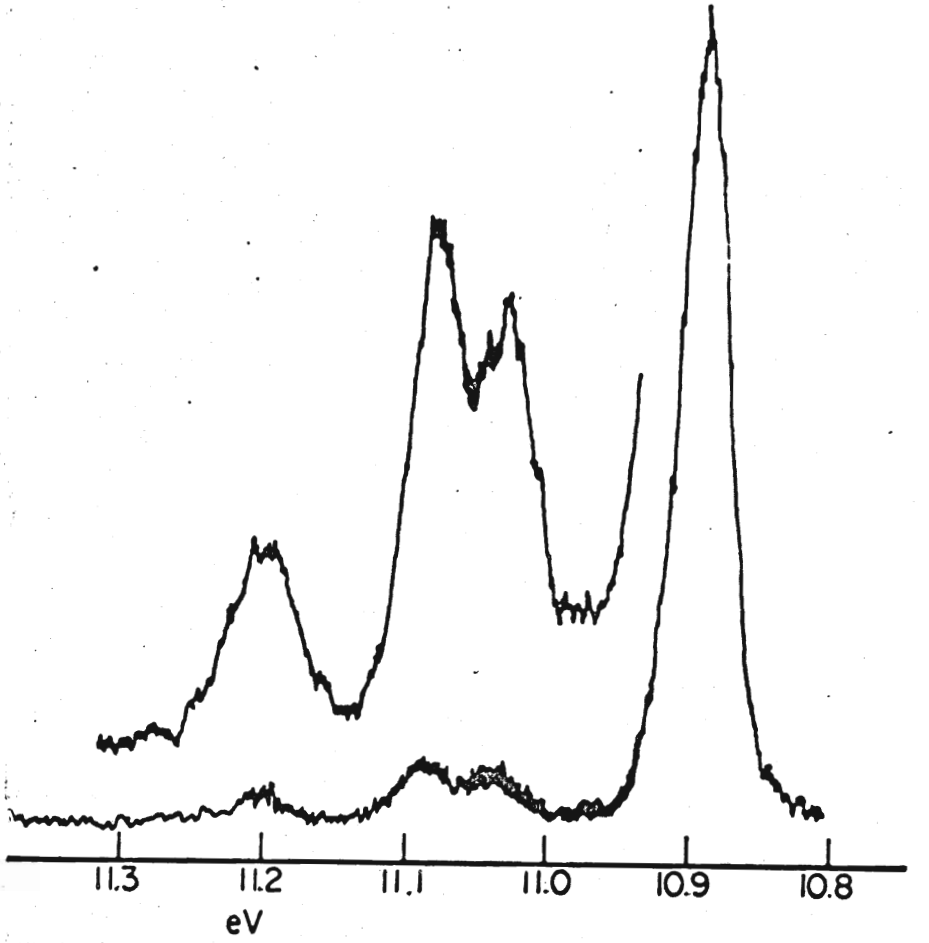

(a)

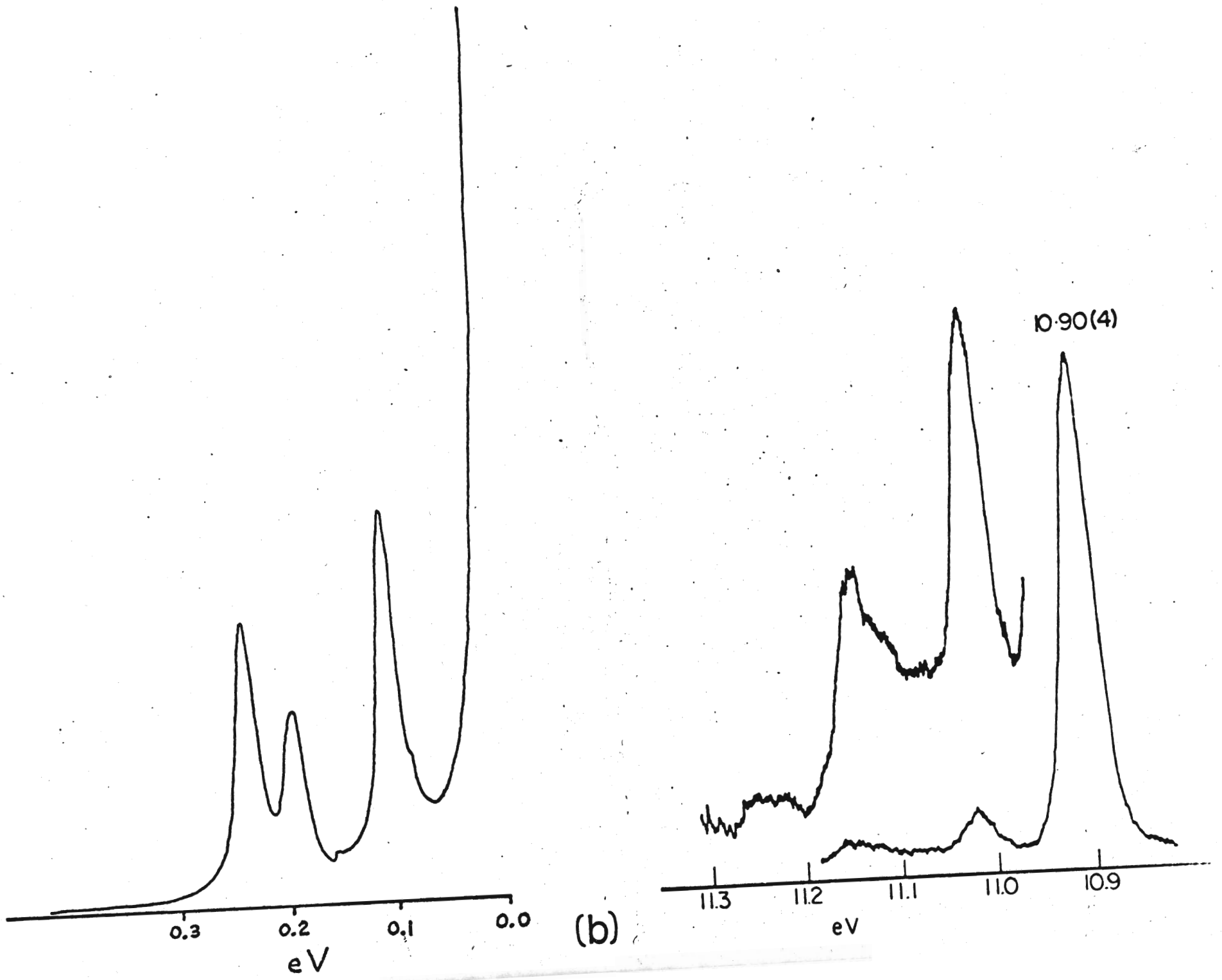
0.3
0.2
0.1
0.0
eV
(b)
10·90(4)
11.3
11.2
11.1
11.0
10.9
eV

(B) $^2B_1(\pi)$ State

The next-highest photoelectron band has been assigned to the $^2B_1(\pi)$ state by Turner, and its origin lies at 14.09 ev. There is a prominent series of bands with a constant spacing of 1210 cm^{-1}. In H_2CO, these bands have an asymmetry in their band envelope to the high frequency side, while D_2CO has a similar asymmetry on the low frequency side. Turner assigned the main progression to the activity of ν_2, the CO stretching frequency. The high frequency satellites in H_2CO were first given the designation 1_o^1, since this was consistent with the observed frequency shift on deuteration.

The results of our CNDO/2 calculations, which are given in Table 6, show that ΔR_{CO}= 0.083 Å, ΔR_{CH} = 0.008 Å, and $\Delta\alpha_{HCH}$ = 4.3°. The large change in carbonyl bond length on ionization is not altogether unexpected, since a four-electron bond is being converted to a three-electron bond in this process. The assignment of the major progression to ν_2 seems to be in keeping with this result. The CNDO/2 results, however, indicate a very small change in the CH bond length on ionization, and hence it is difficult to reconcile Turner's assignment and a frequency shift from 2780 cm^{-1} for $\tilde{X}$ H_2CO to 1400 cm^{-1} for the $^2B_1$ ionic state with this geometry change. As a starting point, we chose the only alternative assignment available, namely 3_o^1, for the satellite bands.

The Franck-Condon structure for this ionic transition was analyzed in a manner analogous to the preceding case. Here the signs of the d's did not present any difficulty since no ambiguities were found in comparing the Mulliken population analysis with the structural changes derived from the calculated potential functions. Since ΔR_{CH} is very small (0.008 Å), d_{CH} would not be expected to contribute to the vibronic

fine structure and would be below the limit of observation. For this reason, ΔR_{CH} was fixed at the CNDO/2 value of 0.008 Å throughout the Franck-Condon fitting procedure. Similarly, k_{CH} was held constant at a value of 4.25 mdyne/Å, and this results in a frequency drop of only 55 cm^{-1} for ν_1.

The results of the fitting procedure are illustrated in Figure 8 and the data is collected together in Tables 5 and 6. The fit to the experimental data does appear to be entirely satisfactory and the spectrum can be interpreted in terms of the activity of two modes alone. The intensity in the 3_o^1 transition which had posed difficulty in the Turner assignment can now be explained by an internal co-ordinate mixing in which the two co-ordinates ΔS_2 and ΔS_3 constructively combine, i.e., $\Delta d_3 = (0.0197)(0.0113) - (0.0045)(0.1320) + (0.0706)(-0.0246)$

Indeed, in this situation, the second term contributes 28% to the total intensity of the 3_o^1 band, and hence this band is three times as strong as that of the $^2B_2(n)$ case even though the structural change in α_{HCH} is only 20% as large.

Figure 8

Comparison of Theoretical and Experimental Results for the $^2B_1(\pi)$ Ionic State

(a) H_2CO (i) Franck-Condon calculation

(ii) experimental

(b) D_2CO (i) Franck-Condon calculation

(ii) experimental

(a)

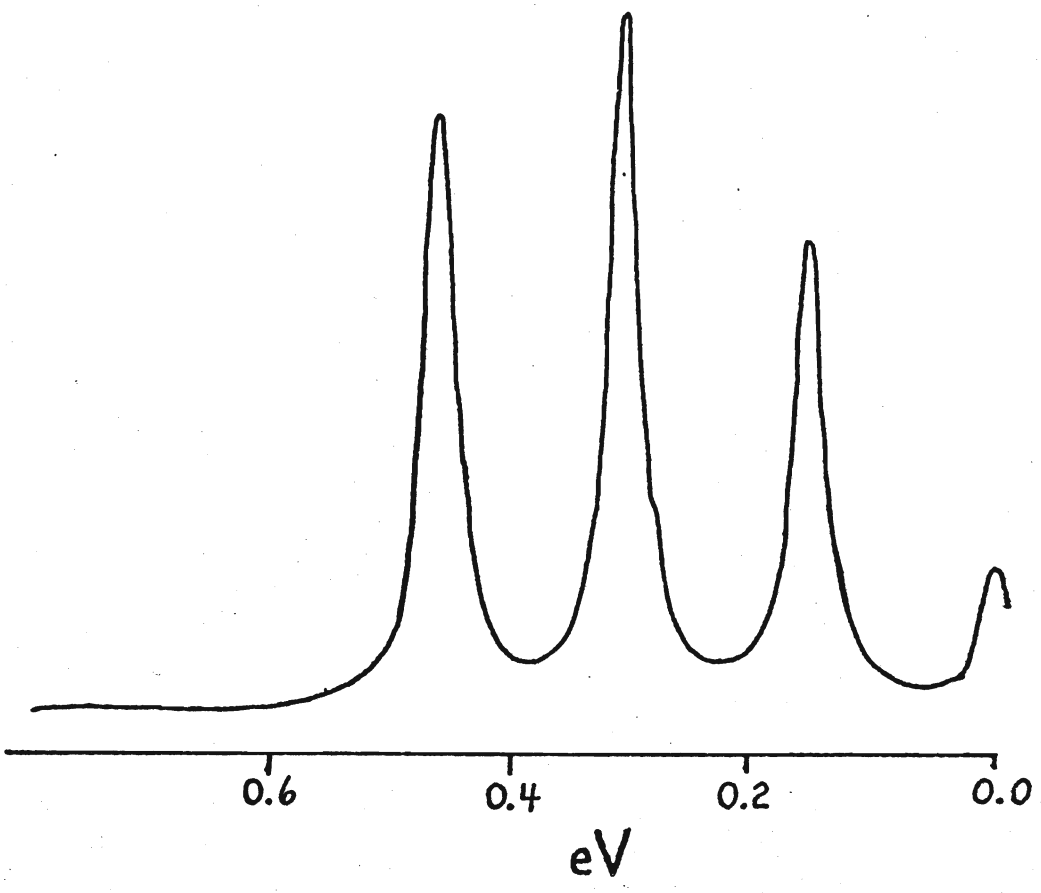

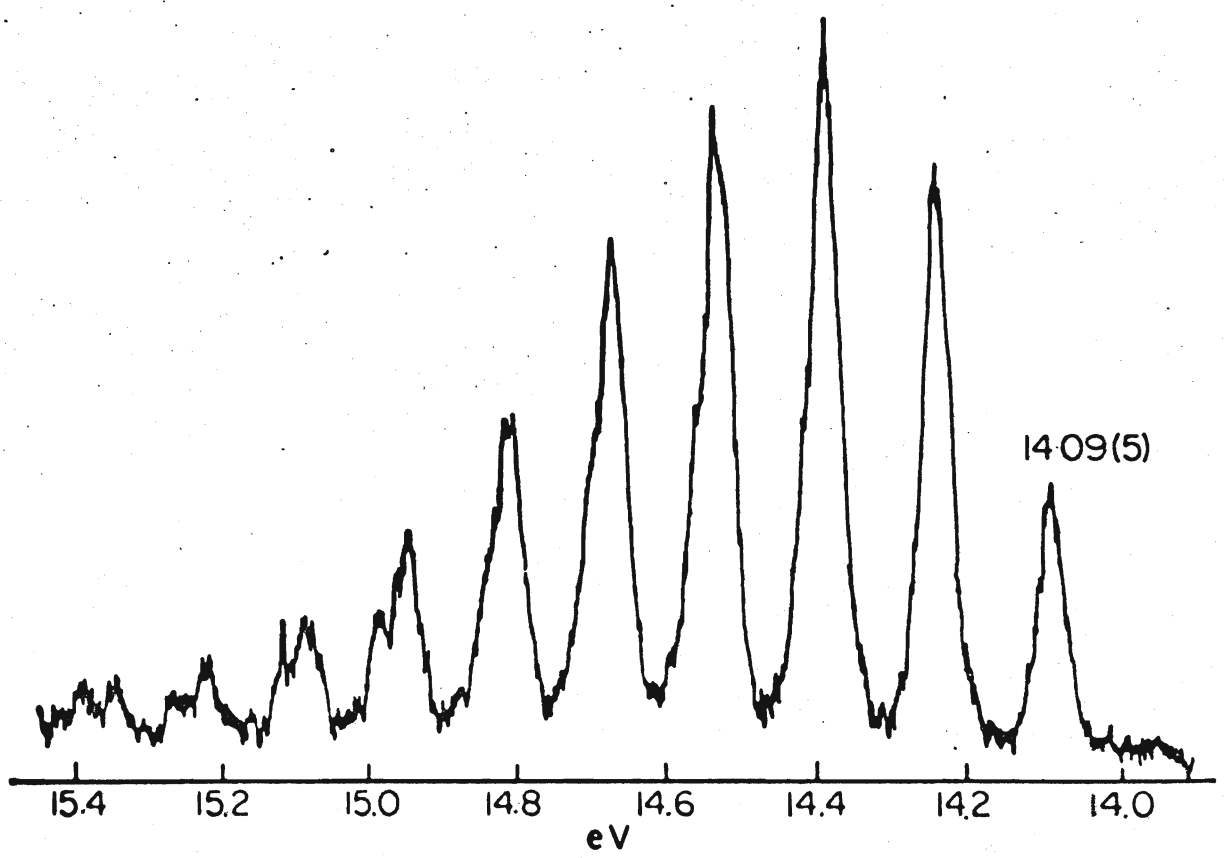

(b)

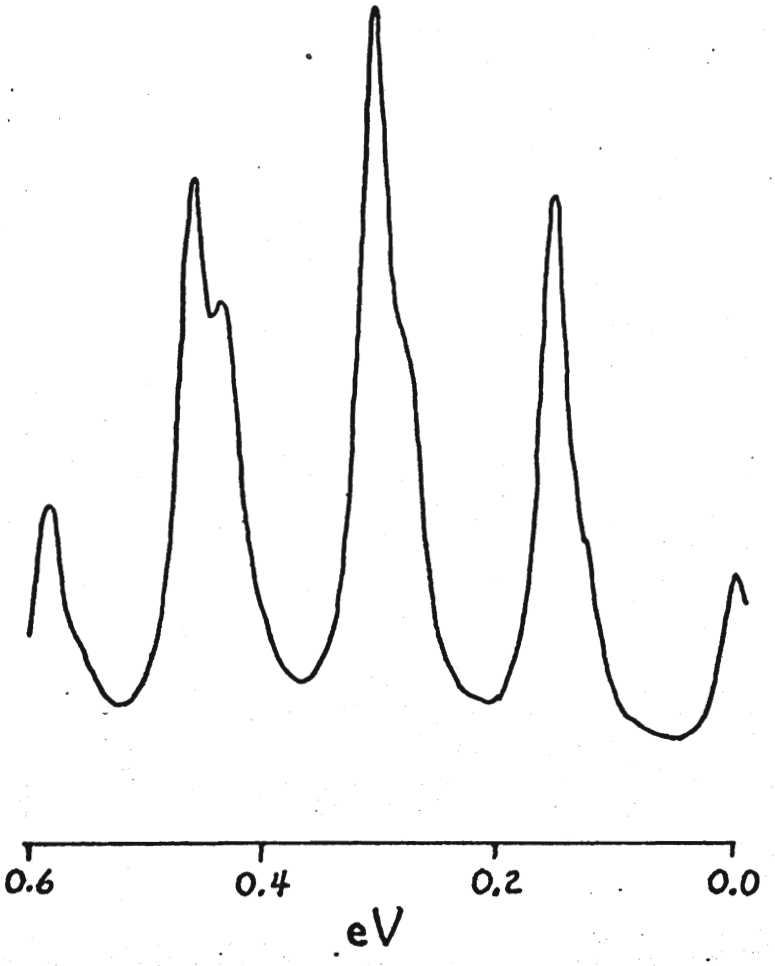

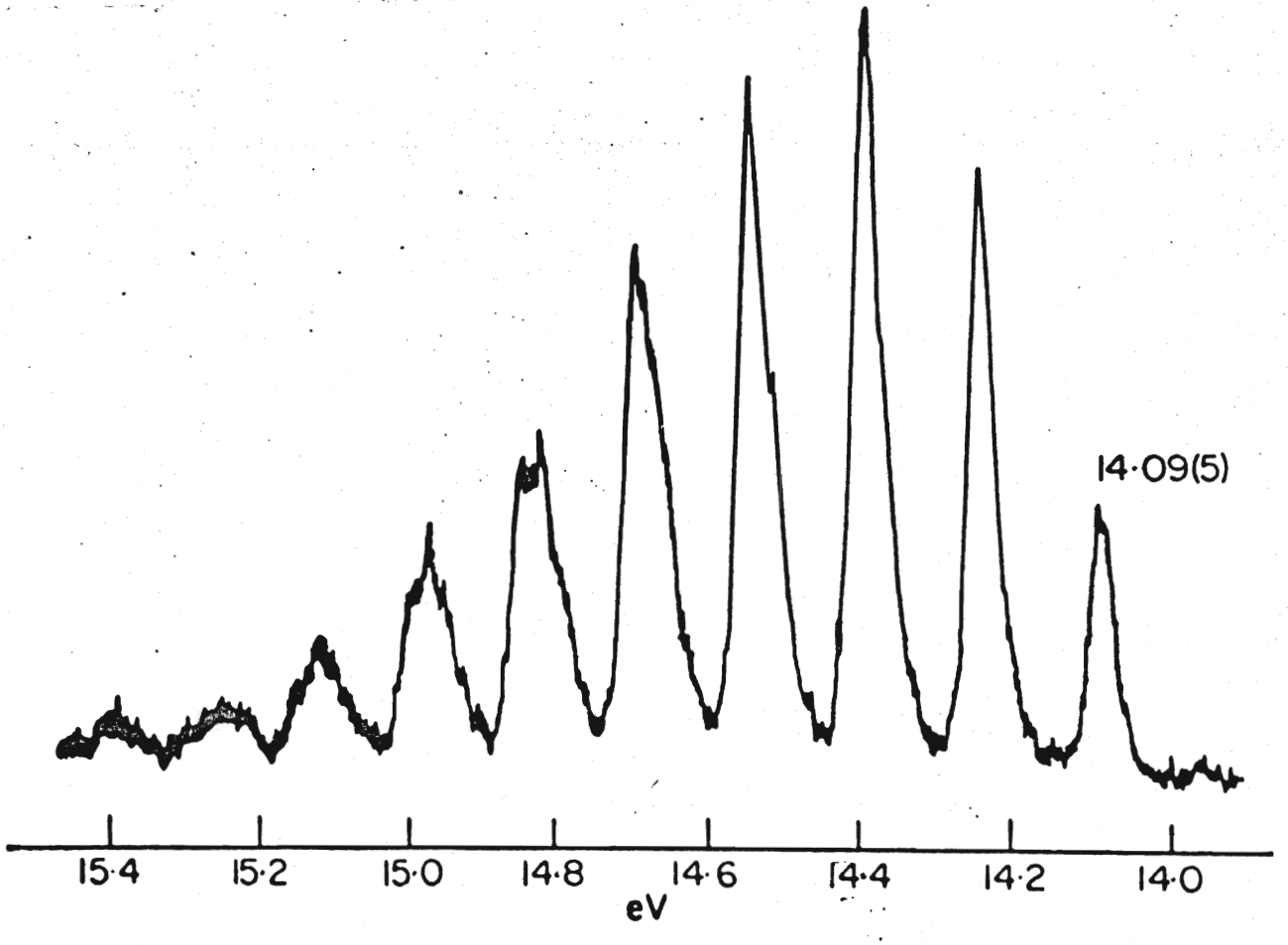

(C) $^2A_1(n\sigma)$ State

The third banded system in the photoelectron spectrum of formaldehyde sets in at 15.84 ev and consists of a series of seven lines which form a progression in an interval of 1270 cm^{-1}. The spectrum of D_2CO, however, clearly shows that at least two modes are active here and are of nearly equal intensity. These frequencies are 1270 and 935 cm^{-1}. Turner assigned the 1270 cm^{-1} frequency on the basis of its invariance to isotopic substitution to ν_2 and the 935 cm^{-1} frequency to ν_3(DCD). The presence of these two modes with seemingly equal strength implies that the ion has been formed by the removal of an electron from an orbital involving bonding over the whole molecule, namely $\sigma_{CH}(b_2)$.

This assignment is not entirely satisfactory for several reasons. The energy of the $\sigma_{CH}(b_2)$ orbital is 2-3 ev below that of the $n\sigma(a_1)$ orbital and therefore Koopman's theorem would predict that ionization should occur from the latter orbital at a lower energy than from the former. In addition, because the HCH bonding is repulsive, loss of an electron from this orbital is expected to cause the angle to close rather than to open; in this case, the frequency of ν_3 should increase from its ground state value of 1500 cm^{-1} (H_2CO).

In view of the important role which internal co-ordinate mixing has played in the analysis of the $^2B_2(n)$ state and the $^2B_1(\pi)$ state, we cannot immediately relate the intensity to the change in a single structural parameter. However, since only two frequencies are active, ν_2 and ν_3, d_1 may reasonably be set equal to zero. In addition, because the intensities of both modes are quite strong, there must be constructive interference such that both d_2 and d_3 have the same sign. From the frequency shifts for ν_2(1746 to 1270 cm^{-1}) and ν_3 (1500 to 1270 cm^{-1}) we conclude that both co-ordinates have expanded on ionic

excitation and that therefore both d_2 and d_3 are positive. With these assignments for d and a set of force constants which reproduced the observed frequencies an excellent fit to the photoelectron profile was obtained, and is illustrated in Figure 9. The data for ΔR_{CO} and $\Delta\alpha_{HCH}$ is contained in Table 6.

To obtain an electronic assignment for this transition, we compared the total energies which were obtained from the CNDO/2 calculations for the following neutral and ionic states: $\tilde{X}^1A_1$, -26.8321 ev; $^2B_2(n)$, -26.3568 ev; $^2B_1(\pi)$, -26.1944 ev; $^2A_1(n\sigma)$, -26.1589 ev. From this the first three ionic states are calculated to be $^2B_2$, $^2B_1$, and $^2A_1$, and should lie at 12.9, 17.3, and 18.3 ev. Turner's observed values of 10.88, 14.09, and 15.84 ev agreed closely with the calculated data, and hence we provisionally assigned the third band to excitation from the $a_1(n\sigma)$ MO.

To test this assignment, it is necessary to compare the results of the Franck-Condon calculations with the corresponding theoretical data obtained for this transition from the CNDO/2 calculations. Our calculated value for the change in HCH angle on ionization is 14° and is in excellent agreement with the CNDO/2 value of 13.8°. Because of the nature of the program, we feel that this is a sensitive criterion and that therefore the assignment of this transition to $n\sigma(a_1)$ ionization is established.

Figure 9

Comparison of Theoretical and Experimental Results for the $^2A_1(n\sigma)$ Ionic State

(a) H_2CO (i) Franck-Condon calculation

(ii) experimental

(b) D_2CO (i) Franck-Condon calculation

(ii) experimental

(a)

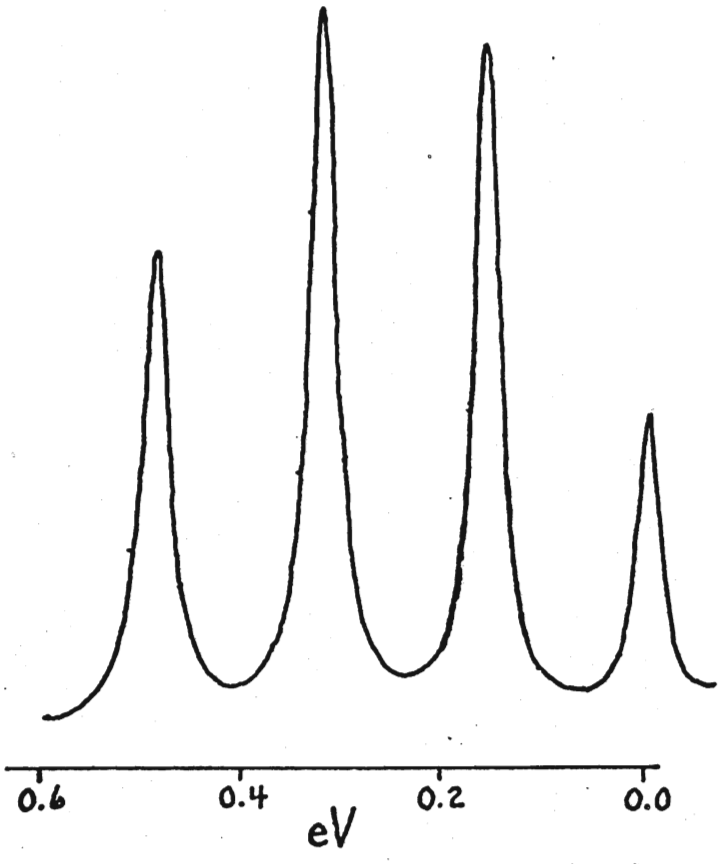

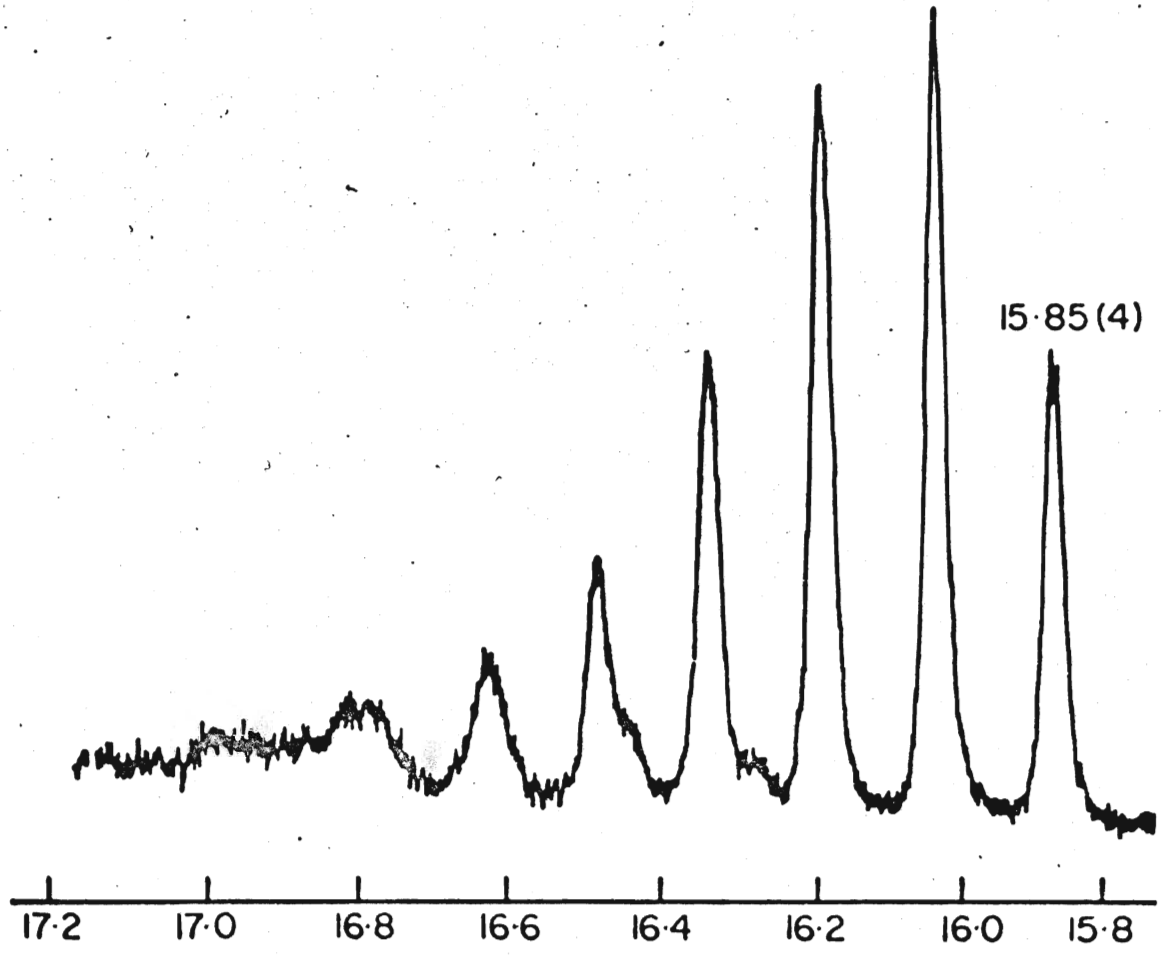

(b)

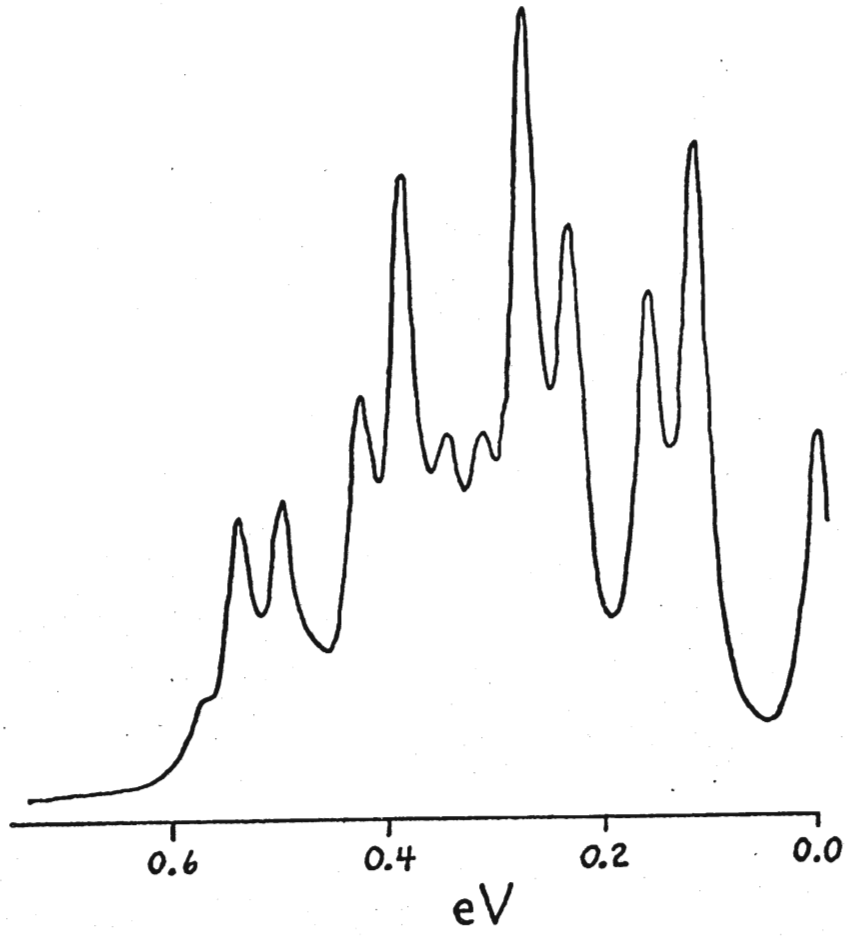

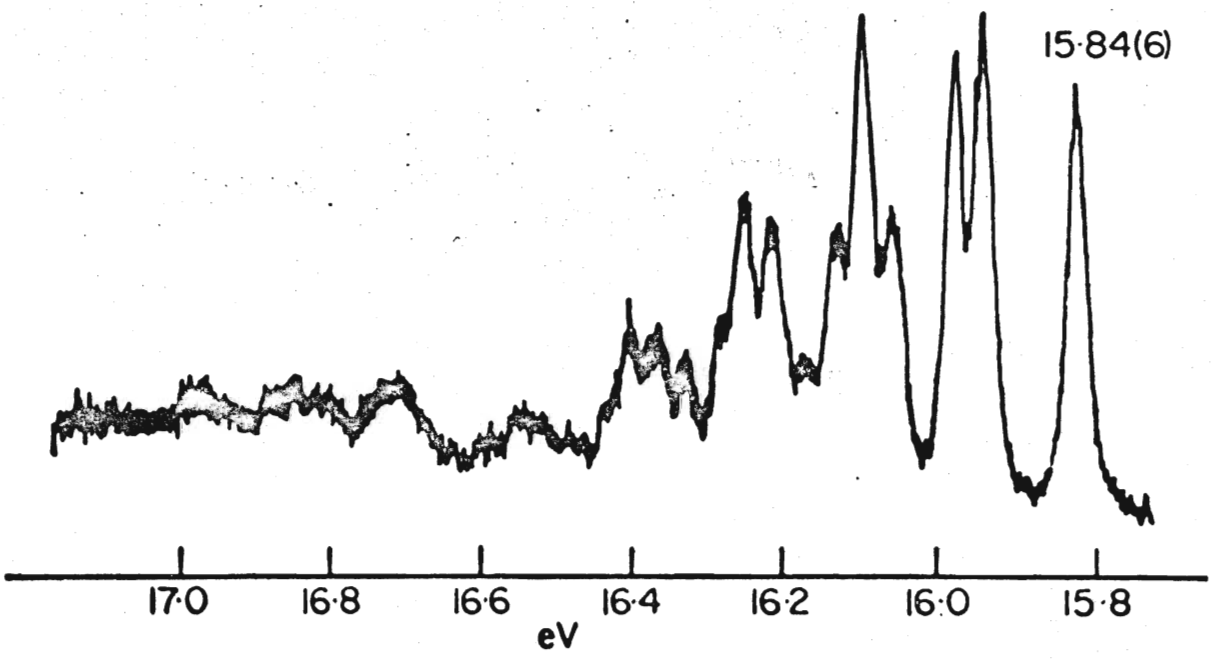

Chapter 5

Rydberg and Intravalence Transitions

The most frequently discussed electronic transitions occuring in the near ultraviolet or visible region of the electromagnetic spectrum involve an electron promotion between two electronic configurations which are derived from orbitals with the same principal quantum number. In the high-energy vacuum ultraviolet region of the spectrum a second type of transition may be observed in which the principal quantum number n changes by 1, 2, 3, ... on excitation. These transitions form a series which terminates for $n = +\infty$ at the ionization limit of the molecule.

Price (28) recorded the spectrum of H_2CO in 1935 in the vacuum ultraviolet region and observed two series of Rydberg transitions. He fitted these into a term value expression which converged at 10.88 ev. and this was taken to be the first ionization limit of formaldehyde. The first series was found to have a quantum defect δ of 0.7 and was assigned to a p series while the second with δ of 0.4 was attributed to a d series. Somewhat later, Allison and Walsh (29) observed this same spectrum under improved conditions of resolution and located a third series with a δ of 1.04 which was assigned to an s series. It is only very recently that interest has been rekindled in the vacuum ultraviolet spectrum of formaldehyde, and this is partly the result of its observation in the interstellar medium (30). Mentall et al (31) photoelectrically recorded the H_2CO spectrum from 2000 Å to the windowless 800 Å region and confirmed much of Walsh and Price's original assignment.

Our results, which were obtained under much improved conditions of resolution for the isotopic species H_2CO, HDCO, D_2CO, and $D_2C^{13}O$ in the

three separate Xe, Kr, and Ar spectral regions, are illustrated in plates 6a, b, and c. Listings of the frequencies may be found in Tables 8,9, and 10 along with vibrational and electronic assignments.

In order to gain more information about the lower members of the Rydberg series in formaldehyde, we executed the modified CNDO program which was described in section B of the theory. Table 4 lists the transition energies which were calculated for a number of Rydberg electronic transitions. The first transition which was obtained in this calculation involves n→3s electron promotion and results in the $^{1,3}B_2$ electronic states. At slightly higher energies, a set of three Rydberg states were obtained which were derived by placing the excited electron in a 3p orbital. These are the $^{1,3}B_2$, $^{1,3}A_1$, and $^{1,3}A_2$ states. Five further lower Rydbergs, the 3d orbitals, also occur, but our calculations are limited to the two Rydberg d states, $^3A_2$ and $^3B_1$.

Similar PCMO calculations have been made by Whitten and Hackmeyer (15) and Buenker and Peyerimhoff (14); both groups used the much more precise ab initio technique of evaluating matrix elements as well as correcting states for configuration interaction (CI). Their results are also listed in Table 4.

The theoretical results discussed above clearly demonstrate that the first allowed transition in the vacuum ultraviolet is the $^1B_2(n,3s) \leftarrow \tilde{X}^1A_1$. This electronic transition may readily be assigned to the intense line-like feature which Allison and Walsh observed at 1750 $\overset{o}{A}$. It should be noted here that most textbooks on spectroscopy-photochemistry erroneously assign this transition to an $n\rightarrow\sigma^*$ electron promotion. The two absorption features which Price observed at slightly higher frequencies can then be assigned from the ab initio calculations to the $^1B_2(n,3p_z) \leftarrow \tilde{X}^1A_1$ and $^1A_1(n,3p_y) \leftarrow \tilde{X}^1A_1$ electronic transitions. The third state, $^1A_2(n,3p_x)$ cannot be

Table 8

Frequencies and Assignments for H_2CO, HDCO, D_2CO, and $D_2C^{13}O$ in the Region from 1800 Å to 1560 Å ($\pm$ 50 cm^{-1})

Assignment	H_2CO		HDCO		D_2CO		$D_2C^{13}O$	
	ν	$\Delta\nu$	ν	$\Delta\nu$	ν	$\Delta\nu$	ν	$\Delta\nu$
			$^1B_2(n,3s) \leftarrow \tilde{X}^1A_1$					
3_1^0	55582	-1581	55915	-1415	56385	-1110		
6_1^0			56302	-1028				
0_0^0	57163		57330		57495		57495	
	57514	+351	57607	+277				
3_0^1	57962	+799	57953	+623	58056	+561	58041	+546
	58744	+1581	58770	+1440	58773	+1278	58771	+1276
1_0^1	59430	+2267	59217	+1887	59192	+1697	59185	+1690
1_0^2	61381	+4218			60840	+3355		
	62386		62297		62179			
	62614	+228						
	62835	+221	62894	+597	62954	+775		
	63087	+252	63152	+258	63105	+151		

Table 9

Frequencies and Assignments for H_2CO, HDCO, D_2CO, and $D_2C^{13}O$ in the Region from 1580 Å to 1329 Å ($\pm$ 20 cm^{-1})

Assignment		H_2CO		HDCO		D_2CO		$D_2C^{13}O$	
		ν	$\Delta\nu$	ν	$\Delta\nu$	ν	$\Delta\nu$	ν	$\Delta\nu$
				$^1A_1(n,3p_y) \leftarrow \tilde{X}^1A_1$					
3_1^0	P	63285	-962	63304	-1033	63347	-1098		
	R	63310	-1005	63387	-1027	63391	-1119		
6_1^1				63567	-807	63688	-789	63621	-839
3_1^1	P					64098	-347	64089	-343
	R					64154	-356	64141	-348
0_0^0	P	64247		64337		64445		64432	
	R	64315		64414		64510		64489	
6_0^1		64546	+265	64612	+238	64658	+181		
6_0^2		64974	+693	64870	+496	64916	+439	64916	+456
3_0^1	P			65219	+882	65149	+704	65173	+741
	R			65268	+854	65209	+699	65215	+726
6_0^3		65451	+1170	65469	+1095	65402	+925	65402	+942
1_0^1				66172	+1798	66169	+1692	66189	+1729
5_0^1				66381	+2007	66283	+1806	66302	+1942
				$^1B_2(n,3p_z) \leftarrow \tilde{X}^1A_1$					
0_0^0		65451		65469					
		65730		65686		65733		65753	
3_0^1		66518	+1067	66381	+912				
		66770	+1040	66666	+980	66508	+775	66525	+772
2_0^1		67130	+1679						
		67279	+1549			67332	+1599	67323	+1570
1_0^1		67472	+2021	67473	+2004				
		67818	+2088	67706	+2020	67547	+1814	67523	+1770

Assignment	H_2CO		HDCO		D_2CO		$D_2C^{13}O$	
	ν	$\Delta\nu$	ν	$\Delta\nu$	ν	$\Delta\nu$	ν	$\Delta\nu$
			$^1B_1(n\sigma,\pi^*) \leftarrow \tilde{X}^1A_1$					
2_0^n	68417		68389		68338		68332	
2_0^{n+1}	69557	+1140			69513	+1175	69501	+1169
2_0^{n+2}	70924	+1367			70805	+1292	70964	+1463
2_0^{n+3}	72229	+1305			72004	+1199	71886	+922
2_0^{n+4}	73400	+1171			73188	+1184	73100	+1214
2_0^{n+5}					74277	+1089	74223	+1123
			Band A					
			69645		69772		69752	
			$^1B_2(n,3d) \leftarrow \tilde{X}^1A_1$					
0_0^0	71507		71566		71541		71599	
3_0^1	72773	+1266	72669	+1103	72506	+965	72550	+951
3_0^2	73926	+2419	73776	+2210	73566	+2025	73394	+1795

Table 10

Frequencies and Assignments for H_2CO, HDCO, D_2CO, and $D_2C^{13}O$ in the Region from 1380 Å to 1215 Å ($\pm$ 50 cm^{-1})

Assignment		H_2CO		HDCO		D_2CO		$D_2C^{13}O$	
		ν	$\Delta\nu$	ν	$\Delta\nu$	ν	$\Delta\nu$	ν	$\Delta\nu$
				$^1B_2(n,4s) \leftarrow \tilde{X}^1A_1$					
0_0^0		74689		74794		74842		74847	
3_0^1		75934	+1245	75859	+1065	75629	+787	75631	+784
2_0^1		76211	+1522			76338	+1496	76264	+1417
1_0^1		76833	+2144			76474	+1632		
$n\rightarrow 4p_y$	P	77240		77348		77390		77404	
	R	77342		77404		77450		77459	
$n\rightarrow 4p_z$		77616		77726		77758		77737	
$n\rightarrow 5s$		80514		80615		80668		80651	
Band B		80820		80899		80955		80964	
$n\rightarrow 5p_y$	P					81845		81862	
	R	81732		81877		81905		81897	
$n\rightarrow 5p_z$						82033		82016	
$n\rightarrow 5d$		82695		82769					
		Rotational Frequencies of Band B ($\pm$ 10 cm^{-1})							
		80803		80862		80939		80923	
		80823	+20	80894	+32	80977	+38	80938	+15
		80859	+36	80930	+36	81012	+35	80947	+9
		80895	+36					80972	+25
								80991	+19
								81016	+25

connected from the ground state by an electric dipole transition, and hence is absent from the spectrum. The higher Rydberg s and p transitions, corresponding to the above, have been observed at 74,689, 77,290, and 77,616 cm^{-1} for n=4 and at 80,514, and 81,732 cm^{-1} for n=5. These experimental energies have been adequately accounted for in the recent ab initio calculations of McKoy (32) and Mentall (31).

(A) $^1B_2(n,4s) \leftarrow \tilde{X}^1A_1$ Transition

Since the dynamics of the Rydberg core are identical to the corresponding ionic states, the photoelectron results should provide useful information about the Rydberg states, and there should be a smooth correlation between the vacuum ultraviolet band profiles and the photoelectron profiles. The n=4 and n=5 Rydbergs appear to be well-behaved in this respect, since it seems feasible in all instances to obtain vibrational assignments, but crowding of the spectra in this region precludes such an analysis. The single exception is the $n \rightarrow 4s$ transition, and here we see an exact image of the $^2B_2$ photoelectron spectrum. There are three weak,broad bands at +787, +1496, and +1632 cm^{-1} from the origin band in the D_2CO spectrum, and these correlate well with the ionic frequencies $\nu_3' = 870$ cm^{-1}, $\nu_2' = 1560$ cm^{-1}, and $\nu_1' = 1910$ cm^{-1}. In H_2CO these bands shift to +1245, +1522, and +2144 cm^{-1}. Again the correlation with the photoelectron spectrum is good, the ionic frequencies being 1210, 1590, and 2560 cm^{-1}.

(B) $^1B_2(n,3p_z) \leftarrow \tilde{X}^1A_1$ Transition

Almost all of the vibrational fine structure associated with the n=3 Rydbergs appears to be subject to forces other than those of the inner core of the molecule, since no 1:1 mapping of the absorption spectra to the photoelectron results can be made. As a starting point for the analysis of these bands, we consider the spectrum of D_2CO, since it is relatively free from the band diffuseness created by predissociation. The $n\rightarrow 3p_z$ transition, which is centred at 65,753 cm^{-1} in D_2CO is the least complex of the n=3 Rydberg transitions. Here the intense origin band has extending to its high frequency side three bands which fit into the same scheme as the ionic transitions. These bands, located at 775, 1599, and 1814 cm^{-1} from the origin, may be assigned respectively to ν_3, ν_2, and ν_1. In HDCO and H_2CO, however, the analysis is not at all clear, partly because of a particularly strong perturbation which has the effect of splitting the origin band in H_2CO into two bands at 65,451 and 65,730 cm^{-1} of nearly equal intensity. Mentall et al (31) had assigned the doublet to the 0^+ and 1^+ levels of a pyramidal formaldehyde, but the present isotope data precludes this assignment, since the doublet character disappears on deuterium substitution. However, the symmetry of this state does allow us to identify the source of the perturbation. The ab initio calculations quoted in Table 3 unequivocally assign this state to the $^1B_2$ representation. For a perturbation to arise from the next lower Rydberg state, which is assigned as $^1A_1$, we require the addition of a vibrational interval of b_2 species. In the H_2CO spectrum, therefore, one of these bands may be assigned to the origin of the $n\rightarrow 3p_z$ transition, as in D_2CO, and the other band to ν_5 or ν_6 quantum additions to the $n\rightarrow 3p_y$ transition. The HDCO spectrum provides verification of this assignment, since the effect of the

perturbation is still quite clearly observed, although the relative intensity has changed with the isotopic shift in frequency and the corresponding change in the strength of the perturbation. The quantum additions to the $^1B_2$ state in H_2CO and HDCO are listed and assigned in Table 9. As these are attached to an origin which is under the influence of a perturbation, the assignments must be regarded as only approximate.

(C) $^1A_1$ $(n,3p_y) \leftarrow \tilde{X}\ ^1A_1$ Transition

The analysis of the Rydberg $n\rightarrow 3p_y$ system has posed a major problem in the study of the vacuum ultraviolet spectrum of formaldehyde. Mentall et al (31) observed that the intense fundamental band at 64,281 cm^{-1} was in fact a doublet with two components of equal intensity separated by 58 cm^{-1}. These they assigned to a pair of transitions terminating on the 0^+ and 0^- vibronic levels of an inversion manifold in ν_4. On deuterium substitution this band preserves its doublet character and the band components vary only slightly in their frequency separation which is not compatible with the prediction of Mentall et al. The infrared spectral studies of Ebers and Nielsen (4a) on D_2CO provide the correct identity of the components. In the infrared these authors observe that the ν_2 type A band at 1700 cm^{-1} possesses well-defined P and R branches with a somewhat weakened central Q branch. The Rydberg transitions in formaldehyde resemble infrared transitions in the sense that relatively small changes in equilibrium structure occur on electronic excitation. The $n\rightarrow 3p_y$ transition here results in an electronic $^1A_1$ state and the transition from the ground electronic state to an excited state would then result in type A polarized bands. The assignment of the doublet feature in the origin bands of H_2CO, HDCO and D_2CO can then be made without equivocation to the P and R rotational branches of a partially resolved type A band.

In the spectrum of D_2CO, type A bands were observed at +757, -347, and -1103 cm^{-1} from the origin band. They are easily identified as each band consists of two components with a constant separation of 50±10 cm^{-1}, and can be fitted into a pattern involving quanta of ν_3 - i.e., 3_0^1, 3_1^1, and 3_1^0. This places ν_3' at 757±20 cm^{-1}, which is to be compared with a ν_3' of 775±20 cm^{-1}

for the nearby $^1B_2$ $(n,3p_z)$ state. A weak progression of bands at +206, +473, and +935 cm^{-1} from the origin can also be identified. These shift to +262, +545, and +1197 cm^{-1} in HDCO and to +411, +683, and +1374 cm^{-1} in H_2CO. It was shown above that the third member of this progression in both the H_2CO spectrum and the HDCO spectrum overlaps and perturbs the origin band of the higher $^1B_2(n,3p_z) \leftarrow \tilde{X}^1A_1$ system. This establishes the symmetry of the vibration as b_2. Positive assignment follows from the identification of the hot band 6_1^1 at -789 cm^{-1} from the origin in D_2CO, since this determines the ground state frequency to be 995 ± 40 cm^{-1}. We can therefore assign the three-membered progression to 6_0^1, 6_0^2, and 6_0^3.

Transitions to odd levels of antisymmetric vibrational eigenstates, such as 6_0^1 and 6_0^3, are forbidden in the electric dipole approximation. However, we have here the necessary conditions for the introduction of the pseudo-Jahn-Teller effect[1]. There are several Rydberg states in close proximity here, namely the 3s, $3p_x$, $3p_y$, and $3p_z$ states, and even the 3d states are within 10,000 cm^{-1}. In addition, there are two nearly degenerate antisymmetric vibrational modes for the formaldehyde molecule, ν_6 at 1251.2 cm^{-1} and ν_4 at 1167.3 cm^{-1}. In this case, the Rydberg states of B_2 symmetry may be perturbed by Rydbergs of A_1 or A_2 symmetry through the interaction of the $Q_6(b_2)$ and $Q_4(b_1)$ vibrational co-ordinates. The Rydberg states of A_1 symmetry may be perturbed by Rydbergs of B_2 symmetry through a $Q_6(b_2)$ interaction or by the single B_1 Rydberg obtained through the $3d_{xy}(a_2)$ electron configuration by a mixing through $Q_4(b_1)$. The $^1A_1(n,3p_y)$ state may therefore interact with the $^1B_2(n,3s)$ state, the $^1B_2(n,3p_z)$ state, the two $^1B_2(n,3d)$ states, and the $^1B_1(n,3d_{xy})$ state. In

---

[1] see appendix B

an effort to predict the shape of the resulting potential function for this state, we employed a double-minimum potential of the Gaussian barrier type. The potential has the form

$$V(Q) = \tfrac{1}{2}\lambda Q^2 + A \exp(-a^2Q^2)$$

This function has been defined by Coon et al (34) and requires three parameters ρ, B, and ν_0 to establish the steepness of the walls, the height of the barrier and the positions of the energy levels. In order to correlate the calculated energy levels with the observed frequency differences in ν_6, it was found necessary to use a very small value of B and to assign a small value to ρ as well. In other words, the potential has almost no barrier, but is broad and has very steep sides. This potential represents the interaction of two opposing forces. The $^1B_2(n,3s)$ state below this state tends to push the walls of the potential function up, while the $^1B_2(n,3d)$ state pushes down on this state, causing the bottom of the well to become very broad and flat.

The best fit to the observed data was obtained with ρ = 0.05, B =0.03 and ν_0 = 886 cm^{-1}. The frequencies evaluated from this potential function for 6_0^1, 6_0^2, and 6_0^3 are 206, 521 and 884 cm^{-1} which are to be compared to the experimental values of 206, 473, and 935 cm^{-1}. To obtain a better fit to the data, this function should be improved by the addition of hexic or octic terms. The height of the barrier separating the equilibrium positions for this function is given as $\nu_0 B$ which is 26 cm^{-1}. This potential is well below the 88 cm^{-1} zero-point energy for this potential function. The implication is clear that the potential has two minima and that in the equilibrium position at either minimum the structural symmetry of the molecule is destroyed and the angle OCH_1 is not equal to OCH_2, which places formaldehyde in the C_s point group. However,

in the zero-point level, which is well above the top of the barrier, the xy symmetry plane has been restored and the C_{2v} symmetry of the molecule is retained.

On the basis of the photoelectron data, the value of ν_3 equal to 870 cm^{-1} for D_2CO would have been anticipated for this state. The observed value of 757 cm^{-1} then is difficult to explain by changes in the electron density of the Rydberg core electrons. A consideration of the valence force field for formaldehyde in this state may provide an explanation here. Since ν_3 and ν_6 are obtained from the same K_{OCH} and K_{HCH} of Wilson's F matrix through symmetric and antisymmetric linear combinations, it would be anticipated that any adjustment of the F matrix to fit ν_6 to a value of 206 cm^{-1} should likewise alter the value of ν_3. The 113 cm^{-1} frequency difference observed between the $^2B_2(n)$ and the $^1A_1(n,3p_y)$ states can be related to the Jahn-Teller coupling which mixes and perturbs the lower Rydberg states of formaldehyde.

The bands which appear at 66,169 and 66,283 cm^{-1} may be assigned to 1_0^1 and 5_0^1 respectively. Again these frequencies are considerably lower than those observed by Turner for the ion. The mechanism responsible for this frequency shift is similar to that described above except that it is the symmetric and antisymmetric combinations of K_{CH_1} and K_{CH_2} which provide the force field for ν_1 and ν_5. Since ν_5 belongs to the same symmetry species as ν_6, it can be affected by pseudo-Jahn-Teller perturbations and ν_1 should alter in value in a parallel manner.

(D) $^1B_2(n,3s) \leftarrow \tilde{X}^1A_1$ Transition

The 3s orbital is the lowest Rydberg orbital observed in the spectrum, and as such its potential function occupies the bottom position in the stack of interacting Rydberg potential functions. However, the $^1B_2(n,3s) \leftarrow \tilde{X}^1A_1$ transition is dominated by a narrow and intense 0 - 0 band as would be expected for a transition which involves electron promotion from a non-bonding orbital to an extra-valence orbital which is essentially non-bonding. From a correlation to the photoelectron spectrum, the assignment of the 1_0^1 and 1_0^2 transitions to broad bands at 2267 and 4218 cm^{-1} in H_2CO is quite straightforward. The corresponding values of 1701 and 3350 cm^{-1} in D_2CO display the correct isotope shift to be given the same assignment. In D_2CO, the hot band 3_1^0 is observed quite clearly at -1104 cm^{-1}. By comparison with the neighbouring $n \rightarrow 3p_y$ transition, we can assign a similar broad band at +561 cm^{-1} to 3_0^1 and hence establish ν_3' as 561 $\pm$ 50 cm^{-1}. Similarly for H_2CO, we can assign 3_1^0 to a band at -1581 cm^{-1} and 3_0^1 to a band at +822 cm^{-1}. In the spectrum of HDCO, there are two hot bands which appear at -1415 and -1028 cm^{-1}. The first band can be readily assigned to 3_1^0, but the appearance of a second band must be explained on the basis of the asymmetry of this molecule. Under the reduced symmetry of the C_s point group, ν_3 and ν_6 both belong to the A' representation, and the band at -1028 cm^{-1} is therefore assigned to 6_1^0.

There remain bands at +351 and +1581 cm^{-1} in the H_2CO spectrum and at +1298 cm^{-1} in the D_2CO spectrum. The key to the vibrational assignment of these bands comes from the large origin isotope shift which is observed among H_2CO, HDCO, and D_2CO. This shift is

three times larger for the n→3s transition than for the n→π* transition; viz 351 and 113 cm^{-1}. It is possible to obtain a rough idea of the changes in vibrational frequency, $\Delta\nu$, on electronic excitation by assuming that the vibrations in the two states are harmonic and then summing the zero-point energies over the six normal modes of H_2CO and D_2CO. If the assumptions are made:

(i) that 3_0^1 is correctly assigned in the D_2CO spectrum

(ii) that the isotopic ratios $\nu(H_2CO)/\nu(D_2CO)$ are identical in the $\tilde{X}^1A_1$ and $^1B_2(n,3s)$ states

(iii) that ν_1' and ν_5', the symmetric and antisymmetric C-H vibrations, suffer the same frequency shift on excitation, the calculation shows that the 351 cm^{-1} origin isotope shift is only compatible with an average downward frequency shift for both ν_4' and ν_6' in H_2CO of 750 cm^{-1}. This effect does not appear in higher members of the n→ns Rydberg series. Indeed, the $^1B_2(n,4s)$ Rydberg at 1340 Å, which has only a 173 cm^{-1} isotope shift, is completely free from the rippling side-band structure which appears on the short wavelength side of the 1750 Å spectra.

The bands at 351 and 1581 cm^{-1} in H_2CO, and at 1298 cm^{-1} in D_2CO then can be attributed to either ν_4 or ν_6. Since the spectrum here is very complex and very diffuse, a more precise statement as to the assignment of these bands cannot be given. What this analysis does demonstrate though is that the $^1B_2(n,3s)$ Rydberg state is strongly mixed into the higher members of the n=3 Rydberg manifold through pseudo-Jahn-Teller interaction. As this state is the lowest state in the Rydberg complex, it would be anticipated that the potential functions for ν_4, ν_5, and ν_6 should all be forced down from the shape that they would assume for the $^2B_2$ ion.

(E) $^1B_2(n,3d) \leftarrow \tilde{X}^1A_1$ Transition

In their original assignments of the vacuum ultraviolet spectrum of formaldehyde, both Price (28) and Allison and Walsh (29) assigned the peak at 1396 Å to an n→3d Rydberg transition, but did not assign the two similar peaks at 1373 Å and 1352 Å. In the work done on the inelastic electron scattering spectrum, Weiss et al (24) assigned the first two lines to separate n→3d transitions, and the question was not resolved even with the increased resolution in Mentall's spectrum (31). Our isotopically labelled spectra completely settle this question. The bands in this region all display the theoretical $\sqrt{2}$ downward frequency shift of the H_2-D_2 isotope substitution and hence the bands must be assigned to vibrational activity in a single electronic state. The 1266 cm^{-1} frequency interval in H_2CO, which falls to 965 cm^{-1} in D_2CO, may be assigned to the ν_3 HCH or DCD bending mode in these two molecules. The ground state values for these two frequencies are 1500.6 and 1105.7 cm^{-1} respectively; in the $^2B_2(n)$ ionic state they assume values of 1242 and 896 cm^{-1}, while in the Rydberg $^1A_1(n,3p_y)$ state ν_3(DCD) has the value of 701 cm^{-1}. The relatively high frequency of ν_3 in this d-type Rydberg state is somewhat unexpected and cannot be glossed over in the analysis. If the Rydberg orbitals could be simply defined as an electronic core which corresponds to the $^2B_2(n)$ ion coupled to an electron which is located in a loose, non-bonding orbital, then we would expect the vibrational frequencies to resemble those of the ionic core. This is not the case, but what is remarkable is the fact that ν_3 for this d Rydberg is shifted upwards in D_2CO by 1106 - 896 = 210 cm^{-1} from the core value while

for the $3p_y$ Rydberg the shift of 896 - 701 = 195 cm^{-1} is opposite and nearly equal. Since the reduction in frequency in the $3p_y$ Rydberg was accounted for by the pseudo-Jahn-Teller effects, the upward shift here can be explained in a similar manner. This 3d Rydberg lies above the 3s and 3p Rydbergs and hence vibronic perturbation effects should shift the potential functions upward. A critical test that this explanation is well-founded comes from consideration of the origin isotope effect. The shift between H_2CO and D_2CO is measured to be 32 cm^{-1} which is very much smaller than that of the 4s Rydberg (173 cm^{-1}) in which no interaction is occurring. We then conclude that in this state quite significant Jahn-Teller coupling is apparent and that it has the opposite effect to that in the 3s and 3p states.

The intensity distribution among 0_0^0, 3_0^1, and 3_0^2 is also perplexing. From the ratio $I(3_0^1)/I(0_0^0)$ we calculate that the change in the Q_3 normal co-ordinate on excitation is $d_3 = -0.03$ $x10^{-20} g^{\frac{1}{2}} cm$. The change in HCH bond angle which is largely responsible for this d value cannot be evaluated directly since a linear combination of the internal co-ordinate changes in R_{CH} and R_{CO} along with the L^{-1} matrix is required. A gross approximation can be made in which only the product $L_{33}^{-1}\Delta S_3$ contributes to d_3. Then the above value of d_3 corresponds to an HCH angle change of either $\pm$ 17°. The discussion on ν_3 intensities in the $^2B_2(n)$ and $^2B_1(\pi)$ ionic spectra, however, demonstrates that this intensity is very sensitive to contributions from the other two internal co-ordinates and hence this angle change can only be regarded as an upper or lower limit to the true value for the change in the HCH bond angle.

(F) $^1B_1(n\sigma,\pi^*) \leftarrow \tilde{X}^1A_1$ Transition

The only intravalence transition which has been definitely assigned in the 1700-1200 Å region is the $^1B_1(n\sigma,\pi^*) \leftarrow \tilde{X}^1A_1$ transition. Table 3, which tabulates the results of both ab initio and semi-empirical calculations, shows that the transition should lie at 1400 Å. Mentall et al (31) were able to observe a series of bands which lay beneath the much stronger Rydberg bands in the region of 1500-1350 Å to which they gave this assignment. It is this system which Sidman (35) made use of to induce intensity into the X-polarized type C bands of the near ultraviolet $n\rightarrow\pi^*$ electronic transition.

Our results show a very broad complex series of diffuse bands in the appropriate region. The absorption coefficients of this system are much lower than the adjacent Rydberg transitions and the spectrum appears to extend over quite a wide spectral region of about 5000 cm^{-1}. Since the band structure in H_2CO is quite different from that in D_2CO, it follows that activity in CH stretching (ν_1, ν_5) or HCH bending (ν_3, ν_4, ν_6) must be present in the spectrum. In addition, the electronic configuration for this state contains a partially filled π^* MO, and it is expected that the molecule is non-planar. Indeed, Peyerimhoff and Buenker (8) have calculated an out-of-plane angle of 7.1° for this state. Such a molecular configuration would have the effect of inducing intensity into the 4_0^2 and 4_0^4 transitions. It is to be anticipated that ν_2 would also be very active in the spectrum, since both the loss of an $n\sigma$ electron and the gain of a π^* electron should substantially reduce the bond order of the carbonyl bond. Our photoelectron calculations show that the loss of an $n\sigma$ electron increases the CO bond length by 0.08 Å while the ν_2 stretching frequency falls from 1746 to 1295 cm^{-1} for H_2CO. The creation

of a partially filled π^* orbital, of which the $n\pi^*$ configuration is a particularly good example, should likewise increase the bond length and reduce the stretching frequency. On $n\rightarrow\pi^*$ excitation, the CO bond length increases by 0.11 Å and ν_2 falls to 1173 cm^{-1}. We therefore expect to see a progression in ν_2 of eight or nine members with the intensity reaching a maximum at v = 4 or 5. In the spectrum of D_2CO, a series of bands is observed. These bands have a rapidly rising intensity profile and a spacing of 1212 $\pm$ 50 cm^{-1}. A similar identification can be made in the spectrum of H_2CO and $D_2C^{13}O$, the frequencies being 1246 $\pm$ 100 cm^{-1} and 1178 $\pm$ 100 cm^{-1} respectively. The small frequency shift on deuteration establishes the assignment of this progression to ν_2, the CO stretching frequency. The $D_2C^{13}O$ spectra prove to be useful here, since the isotope shift on C^{12}- C^{13} substitution is sufficiently small for a correlation to be made. A line at 73,188 cm^{-1} in D_2CO was found to shift to 73,100 cm^{-1} in $D_2C^{13}O$. With the vibrational frequency shift of 24 cm^{-1}, this isotope effect of 88 cm^{-1} may be used to obtain the numbering of the vibrational quanta in the CO mode. That is, if we assume no origin isotope effect, the 73,188 cm^{-1} band must be given the assignment 2_0^4. When a reasonable C^{12}- C^{13} origin shift is incorporated into this calculation, a more probable assignment for this band would be 2_0^6 or $X2_0^6$, where X represents even quanta of ν_4'. This would place the origin in the region of 65,000 to 66,000 cm^{-1}, and it appears to be buried beneath the $n\rightarrow 3p$ Rydberg transitions.

At 2000 cm^{-1} to lower frequencies from this electronic origin, several bands are observed in the spectrum of H_2CO, HDCO, and D_2CO with very sharp rotational profiles. The wavenumber values of these bands do not fit into the vibrational scheme of the $^1A_1(n,3p_y)$ Rydberg bands and their band envelopes are totally different from the Rydberg bands at higher

frequencies. From all indications, these bands resemble those of an intravalence transition. All of the theoretical work to date, however, has predicted only one intravalence band in this region, namely the $n\sigma \rightarrow \pi^*$ transition. Our $C^{12} - C^{13}$ isotope effect studies, on the other hand, indicate that these bands cannot be associated with $n\sigma \rightarrow \pi^*$. Either we are observing here a new phenomenon which cannot be accounted for by existing MO theory or our vibrational assignments for the $n\sigma \rightarrow \pi^*$ transition have to be adjusted by quantum additions of 2000 cm^{-1}.

(G) Band A

There is a band which appears at 69,892 cm^{-1} in D_2CO and 69,728 cm^{-1} in HDCO as a weak but quite sharp feature. From the shift of the underlying $n\sigma \rightarrow \pi^*$ transition with $C^{12}-C^{13}$ isotopic substitution we can eliminate the possibility that this is an intravalence transition. The 127 cm^{-1} HD-D_2 isotope effect and the lack of associated vibrational fine structure indicate that this is a Rydberg transition resulting from the promotion of the b_2 non-bonding electron. The direction of the isotope shift establishes that this is the 0-0 origin band of the Rydberg transition. Since this spiky band lies between the 3d band and the pair of 3p Rydberg bands, it could be given two assignments. This band could be the missing $3p_x$ Rydberg component which cannot combine under electric dipole radiation with the ground electron configuration in which case the band would have to be magnetic dipole allowed. This possibility seems to be overruled, however, because of intensity considerations. A better assignment for this band is to a Rydberg 3d state. Under the influence of the C_{2v} electric field, the five 3d Rydberg orbitals decompose into the direct sum $\Gamma = 2a_1 \oplus a_2 \oplus b_1 \oplus b_2$ which results in the corresponding $^1A_1$, $^1A_2$, $^1B_1$, and two $^1B_2$ states. Since a transition to the $^1A_2$ state is forbidden, only three possibilities exist for this assignment. Once again, the origin isotope shift is of value here, since the effect is quite large, and hence it appears that this state is also undergoing pseudo-Jahn-Teller perturbation from a higher state. As the strongly allowed transition at 8.94 ev is assigned to $^1B_2(n,3d) \leftarrow \tilde{X}^1A_1$, a b_2 vibronic mechanism would lead to the assignment $^1A_1(n,3d) \leftarrow \tilde{X}^1A_1$ for this transition. It was possible to obtain a satisfactory fit of a calculated rotational band contour to the observed contour of the band using type A rotational selection rules

and setting $\Delta A = \Delta B = \Delta C = 0$. This rotational selection rule does support the above electronic assignment. However, it should be recognized that it is possible to obtain rotational contours with a spiky appearance from type B or type C rules where large values of ΔA are involved. Further analysis of the Rydberg bands in this region must await a serious ab initio MO calculation designed specifically for the 3d Rydbergs, similar to those of Buenker and Peyerimhoff (14) and Whitten and Hackmeyer (15).

(H) Band B

There is an unusual band which appears in the spectrum of H_2CO at 1235 Å, designated B in Figure 6c. The isotope shift of this band is 120 cm^{-1} between H_2CO and D_2CO, and the system consists of a single broad band with several narrow bands closely spaced to the high frequency side. These lines have a constant spacing of 36 ± 10 cm^{-1} in H_2CO, and this evidence leads us to assign these lines to the rotational structure of an electronic transition in formaldehyde. Isotopic evidence indicates that the active mode involves hydrogenic motion, but there is no indication of vibrational activity, which suggests either a very small change in geometry or predissociation of the molecule.

Using the Parkin band contour program, we attempted to synthesize the rotational band envelope and structure of this band from the available information. The shape of the band envelope suggests a perpendicular band, and the degradation of the structure to the blue requires that A' be greater than A". With these conditions, it is possible to obtain an approximate fit to the experimental data, and the change in the HCH angle on excitation is calculated to be -5^{o}. Nevertheless, while some information about the equilibrium structure and the direction of the polarization of the transition is known, the assignment of the electronic eigenstate is not forthcoming. This, however, is a common feature in the analysis of band systems in the high Rydberg region of the spectrum. In the case of formaldehyde, where excellent ab initio calculations are tractable, no doubt an answer will be available to this question in the near future.

References

1. R. W. B. Pearse, "The Identification of Molecular Spectra", Chapman and Hall, Limited, (London, 1941)

2. R. S. Mulliken, J. Chem. Phys., 23, 1997 (1955)

3. K Takagi and T. Oka, J. Phys. Soc. Japan, 18, 1174 (1963).

4. (a) E. S. Ebers and H. H. Nielsen, J. Chem. Phys., 6, 311 (1938)
   (b) H. H. Blau, Jr., and H. H. Nielsen, J. Mol. Spectr., 1, 124 (1957)
   (c) J. R. Patty and H. H. Nielsen, Phys. Rev., 39, 957 (1932)
   (d) D. W. Davidson, B. I. Stoicheff, and H. J. Bernstein, J. Chem. Phys., 22, 289 (1954)
   (e) T. Nakagawa, K. Kashiwagi, H. Kurihara, and Y. Morino, J. Mol. Spectr., 31, 436 (1969)

5. V. A. Job, V. Sethuraman, and K. K. Innes, J. Mol. Spectr., 30 365 (1969)

6. A. D. Walsh, J. Chem. Soc., 2306 (1953)

7. J. C. D. Brand, J. Chem. Soc., 858 (1956)

8. R. J. Buenker and S. D. Peyerimhoff, J. Chem. Phys., 53, 1368 (1970)

9. (a) J. A. Pople, D. P. Santry, and G. A. Segal, J. Chem. Phys., 43, S129 (1965)
   (b) J. A. Pople and G. A. Segal, J. Chem. Phys., 43, S136 (1965)
   (c) J. A. Pople and G. A. Segal, J. Chem. Phys., 44, 3289 (1966)

10. S. R. LaPaglia, J. Mol. Spectr., 10, 240(1963)

11. D. R. Salahub and C. Sandorfy, Theor. Chim. Acta, 20, 227 (1971)

12. R. S. Mulliken, J. Am. Chem. Soc., 86, 3183 (1964)

13. T. C. Betts and V. McKoy, J. Chem. Phys., 60, 2947 (1974)

14. S. D. Peyerimhoff, R. J. Buenker, W. E. Kammer, and H. Hsu, Chem. Phys. Letters, 8, 129 (1971)

15. J. L. Whitten and M. Hackmeyer, J. Chem. Phys., 51, 5584 (1969)

16. R. S. Mulliken, J. Chem. Phys., 23, 1833 (1955)

17. H. W. Kroto and R. D. Santry, J. Chem. Phys., 47, 792,2736 (1967)

References (cont'd)

18. E. B. Wilson, Jr., J. C. Decius, and P. C. Cross, " Molecular Vibrations ", McGraw-Hill, New York (1955)

19. T. Shimanouchi and I. Suzuki, J. Chem. Phys., 42, 296 (1965)

20. J. B. Coon, R. E. deWames, and C. M. Loyd, J. Mol. Spectr., 8, 285 (1962)

21. (a) G. Herzberg and E. Teller, Z. Phys. Chem., B21, 410 (1933)
(b) H. Sponer and E. Teller, Revs. Mod. Phys., 13, 75 (1941)
(c) E. U. Condon, Am. J. Phys., 24, 1104 (1956)

22. F. Ansbacher, Z. Naturforsch, 14a, 889 (1959)

23. A. D. Baker, C. Baker, C. R. Brundle, and D. W. Turner, Intern. J. of Mass Spectrom. and Ion Phys., 1, 285 (1968)

24. M. J. Weiss, C. E. Kuyatt, and S. Mielczarek, J. Chem. Phys., 54, 4147 (1971)

25. A. Chutjian, J. Chem. Phys., 61, 4279 (1974)

26. D. W. Turner, Proc. Royal Soc. London A, 307, 15 (1968)

27. D. W. Turner, C. Baker, A. D. Baker, and C. R. Brundle, " Molecular Photoelectron Spectroscopy ", Wiley Interscience (1970) p. 141-150

28. W. C. Price, J. Chem. Phys., 3, 256 (1935)

29. K. Allison and A. D. Walsh, Chemical Institute of Canada Symposium, Ottawa,1957

30. L. E. Snyder, D. Buhl, B. Zuckerman, and P. Palmer, Phys. Rev. Letters, 22, 679 (1969)

31. J. E. Mentall, E. P. Gentieu, M. Krauss, and D. Neumann, J. Chem. Phys., 55, 5471 (1971)

32. D. L. Yeager and V. McKoy, J. Chem. Phys., 60, 2714 (1974)

33. M. K. Orloff and N. B. Colthup, J. Chem. Ed., 50, 400 (1973)

34. G. Herzberg, " Electronic Spectra of Polyatomic Molecules ", D. Van Nostrand Co., Inc., (Princeton, 1967)

35. R. M. Hochstrasser and C. A. Marzzacco, " Molecular Luminescence ", ed. E. C. Lim, Benjamin (New York, 1969)

References (cont'd)

36. J. B. Coon, N. W. Naugle, and R. D. McKenzie, J. Mol. Spectr., 20, 107 (1966).

37. J. A. Pople and J. W. Sidman, J. Chem, Phys., 27, 1270 (1957).

38. I. Absar, C. S. Lin, and K. L. McEwen, Can. J. Chem., 50, 646 (1972).

39. R. L. Ellis, R. Squire, and H. H. Jaffé, J. Chem. Phys., 55, 3500 (1971).

40. T. Anno and A. Sado, J. Chem. Phys., 26, 1759 (1957).

41. J. W. Sidman, J. Chem. Phys., 27, 429 (1957).

42. J. C. Ho, G. A. Segal, and H. S. Taylor, J. Chem. Phys., 56, 1520 (1972).

43. C. Giessner-Prettre and A. Pullman, Theor. Chim. Acta, 18, 14 (1970).

44. T. H. Dunning and V. McKoy, J. Chem. Phys., 47, 1735 (1967).

45. J. L. Whitten, J. Chem. Phys., 56, 5458 (1972).

46. C. R. Lessard, D. C. Moule, and S. Bell, Chem. Phys. Letters, 29, 603 (1974).

Appendix A

Mulliken Overlap Population

In 1955, Mulliken (16) presented a new method for an analysis in semi-quantitative form of the breakdown of the electronic population of molecules into partial and gross atomic populations or into partial and total net populations together with overlap populations. Gross populations distribute the electrons almost perfectly among the AO's of the various atoms in the molecule. The overlap population for any pair of atoms in a molecule is in fact made up of positive and negative contributions. If the overlap population between two atoms is positive, they are bonded; if negative, they are antibonded.

Consider any normalized MO, ϕ_i, of a polyatomic molecule, written in approximate form as a linear combination of normalized AO's, χ_r, of the atom K:

$$\phi_i = \sum_{r_k} c_{ir_k} \chi_{r_k}$$

If the MO is occupied by N electrons (usually N = 2) this population may be considered as divided into subpopulations whose detailed distributions in space are given by the terms in the following expression:

$$N(i) = N(i)\sum_{r_k} c_{ir_k}^2 + 2N(i)\sum_{\ell > k} c_{ir_k} c_{is_\ell} S_{r_k s_\ell}$$

where $S_{r_k s_\ell}$ is the overlap integral $\int \chi_r \chi_s dv$.

The various terms represent different partial and subtotal overlap populations corresponding to various degrees and kinds of breakdown of a total overlap population. The overlap which is of interest to us is the following:

$$n(i) = \sum_{r_k} \sum_{s_\ell} c_{ir_k} c_{is_\ell} S_{r_k s_\ell}$$

The following example, taken from the CNDO printout for the ground state σ_{CO} orbital, may clarify this method of calculation.

Atomic Orbital			Orbital Coefficients	Overlap Integrals	
1	H	s	-0.1397	S_{12}	0.1547
2	H	s	-0.1397	S_{13}	0.5044
3	C	s	-0.4835	S_{16}	-0.2523
4	C	p_x	-0.0000	S_{17}	0.0783
5	C	p_y	-0.0000	S_{110}	-0.0706
6	C	p_z	-0.2996	S_{37}	0.3798
7	O	s	-0.7804	S_{310}	-0.3103
8	O	p_x	0.0000	S_{67}	0.4637
9	O	p_y	0.0000	S_{610}	-0.3053
10	O	p_z	0.1684		

Then $n_{CO} = \sum_{ij} c_{iC} c_{jO} S_{ij}$

$n_{CH} = \sum_{i} c_{iC} c_{H} S_{i1}$

$n_{OH} = \sum_{j} c_{jO} c_{H} S_{j1}$

$n_{HH} = c_{H} c_{H} S_{12}$

In order to obtain the overlap population between a pair of atoms, it is only necessary to multiply these numbers by the number of electrons in the molecular orbital, and hence we have the following overlap populations for the σ_{CO} orbital in the ground state:

CO	+0.5854
CH	+0.0476
OH	+0.0206
HH	+0.0062

Appendix B

The Jahn-Teller Effect

In the Born-Oppenheimer approximation, the electronic wavefunctions of a molecule are completely orthogonal to each other. However, in the presence of antisymmetric vibrational motion, mixing between the states is possible which may be attributed to the breakdown of the Born-Oppenheimer approximation. This interaction has three forms, known as the Jahn-Teller, Herzberg-Teller, or Renner-Teller effects, depending on the structure of the molecule and its electronic state (34). The particular effect which is of revelance to our work is the pseudo-Jahn-Teller effect, which pertains to a non-linear polyatomic molecule with two nearly degenerate electronic states and two nearly equal vibrational frequencies. The electronic symmetry of the two states need not agree, but the total vibronic symmetry (i.e. the direct product of the representation of the vibrational and the electronic wavefunctions) must agree. Therefore, the distortion occurs only as a function of certain normal co-ordinates, and the magnitude of the interaction varies inversely with the separation of the unperturbed levels.

In particular, for a molecule of C_{2v} symmetry, such as H_2CO, the following interactions are possible:

A_1 and B_1 via b_1	A_2 and B_1 via b_2
A_1 and B_2 via b_2	A_2 and B_2 via b_1
B_1 and A_1 via b_1	B_2 and A_1 via b_2
B_1 and A_2 via b_2	B_2 and A_2 via b_1

The net effect of this interaction is to force the lower potential function down into a double-minimum configuration and the higher potential up into a steep-sided configuration, although in both cases the origin does not change in energy. The vibrational frequency connected with the normal co-ordinate which permits interaction will also be affected, so that the frequency in the lower state drops drastically from its ground state value, while in the upper state it increases noticeably. This effect is illustrated in Figure 10a.

A useful theoretical description of this vibronic interaction between two electronic states has been developed by Hochstrasser (35), who uses a Hamiltonian of the form

$$H(Q) = H_o(Q_1) + \sum_a \left(H'(Q_1)\right) \Delta Q_a + \tfrac{1}{2}\sum\sum_{ab} \left(H''(Q_1)\right) \Delta Q_a \Delta Q_b$$

where $H_o(Q_1)$ is the Hamiltonian at a fixed point Q_1, and the other two terms correct for interaction between the vibrational and electronic wavefunctions. If we assume that there are only two electronic states involved, that the two electronic wavefunctions are of different symmetry, and that the normal co-ordinates in the two states are identical, then we have the following 2x2 matrix:

$$\begin{bmatrix} \langle 1|H|1\rangle & \langle 1|H|2\rangle \\ \langle 2|H|1\rangle & \langle 2|H|2\rangle \end{bmatrix}$$

where 1 and 2 denote the two electronic wavefunctions. Diagonalization of this matrix for a particular value of Q results in a pair of eigenvalues ε_1 and ε_2 such that

$$\varepsilon^{(1)}_{1,2}(Q) = \varepsilon^{(1)}_{av.}(Q) \pm \tfrac{1}{2} \left\{\Delta\varepsilon^2_{12} + 4\left[\sum_n v_{12}(n)\Delta Q_n + \tfrac{1}{2}\sum\sum_{ab} v_{12}(a,b)\Delta Q_a \Delta Q_b\right]^2\right\}^{\frac{1}{2}}$$

where $\Delta\varepsilon_{12} = \varepsilon_1(Q) - \varepsilon_2(Q)$

$$\sum_n v_{12}(n)\Delta Q_n = \sum_n \langle 1 \left| \left(\frac{\partial H_o(Q)}{\partial Q_n}\right)_{Q_1} \right| 2\rangle \Delta Q_n$$

$$\sum_{ab} v_{12}(a,b)\Delta Q_a \Delta Q_b = \sum_{ab} \langle 1 \left| \left(\frac{\partial^2 H_o(Q)}{\partial Q_a \partial Q_b} \right)_{Q_1} \right| 2 \rangle \Delta Q_a \Delta Q_b$$

$$\varepsilon^{(1)}_{av.}(Q) = \tfrac{1}{2}\sum_i \{\varepsilon^{(1)}_i + \sum_s v_{ii}(s)\Delta Q_s + \tfrac{1}{2}\sum_{ab}\sum v_{ii}(a,b)\Delta Q_a \Delta Q_b\}$$

Thus, for a fixed vibronic interaction v_{12}, it is possible to generate a series of potential energy curves for various energy gaps, as shown in Figure 10b.

This model may be extended to the situation where three or more electronic states interact vibronically with each other. However, as the size of the matrix and the number of off-diagonal elements increases, the problem cannot be handled analytically and a numerical analysis is required.

Figure 10

The Jahn-Teller Effect

---- Unperturbed Potential Functions

——— Potential Functions Perturbed By Interaction Through the Normal Co-ordinate Q_i

(a) Pseudo-Jahn-Teller Effect for Molecules with two Electronic States which are nearly degenerate

(b) Calculated Potential Energy Curves for a fixed Vibronic Interaction $v_{12}(n)$ of 5×10^3 $cm^{-1}(\text{A}^{\circ})^{-1}$ and at various Energy Gaps (ref. 35)

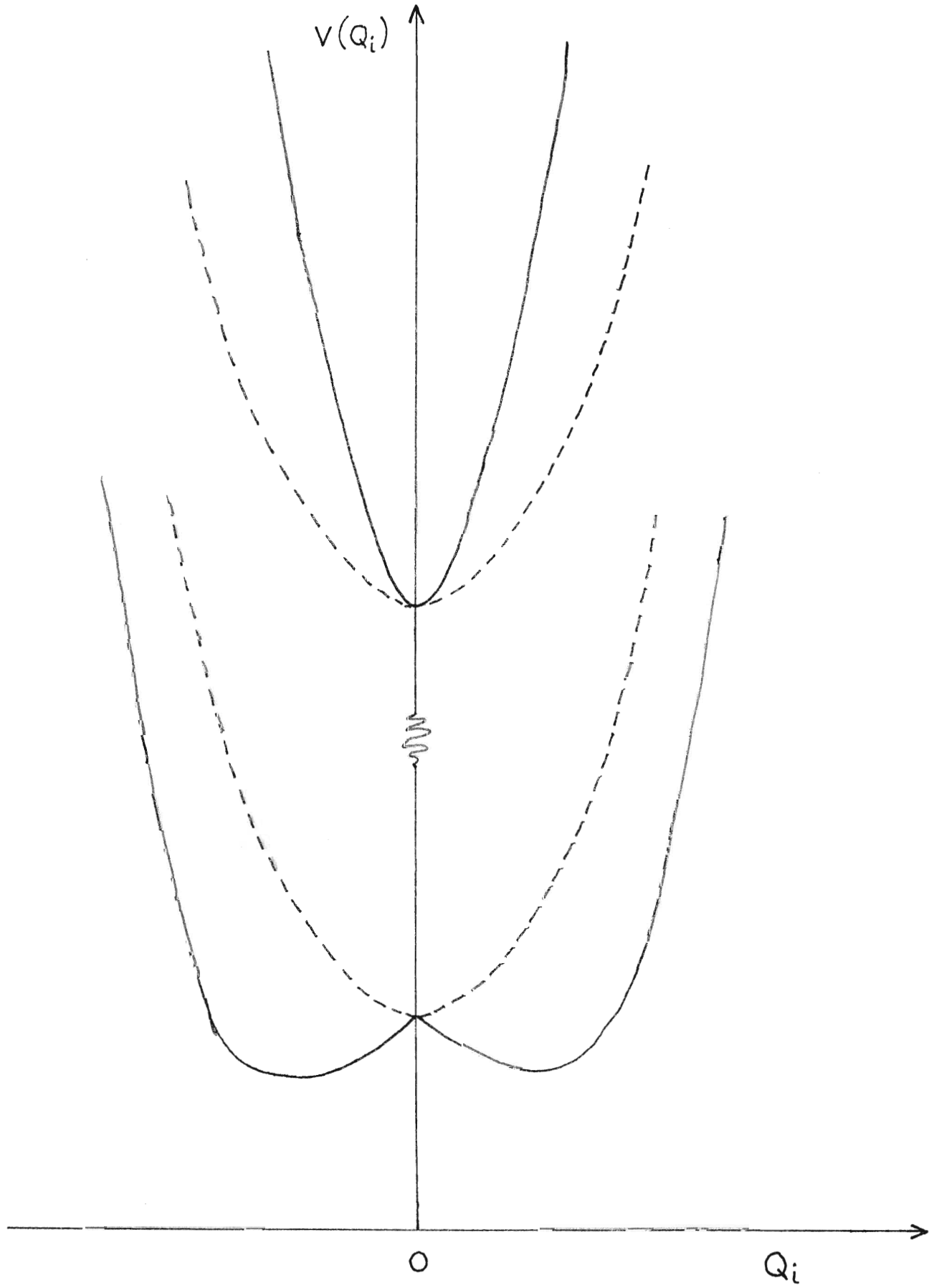
V(Qi)
0
Qi

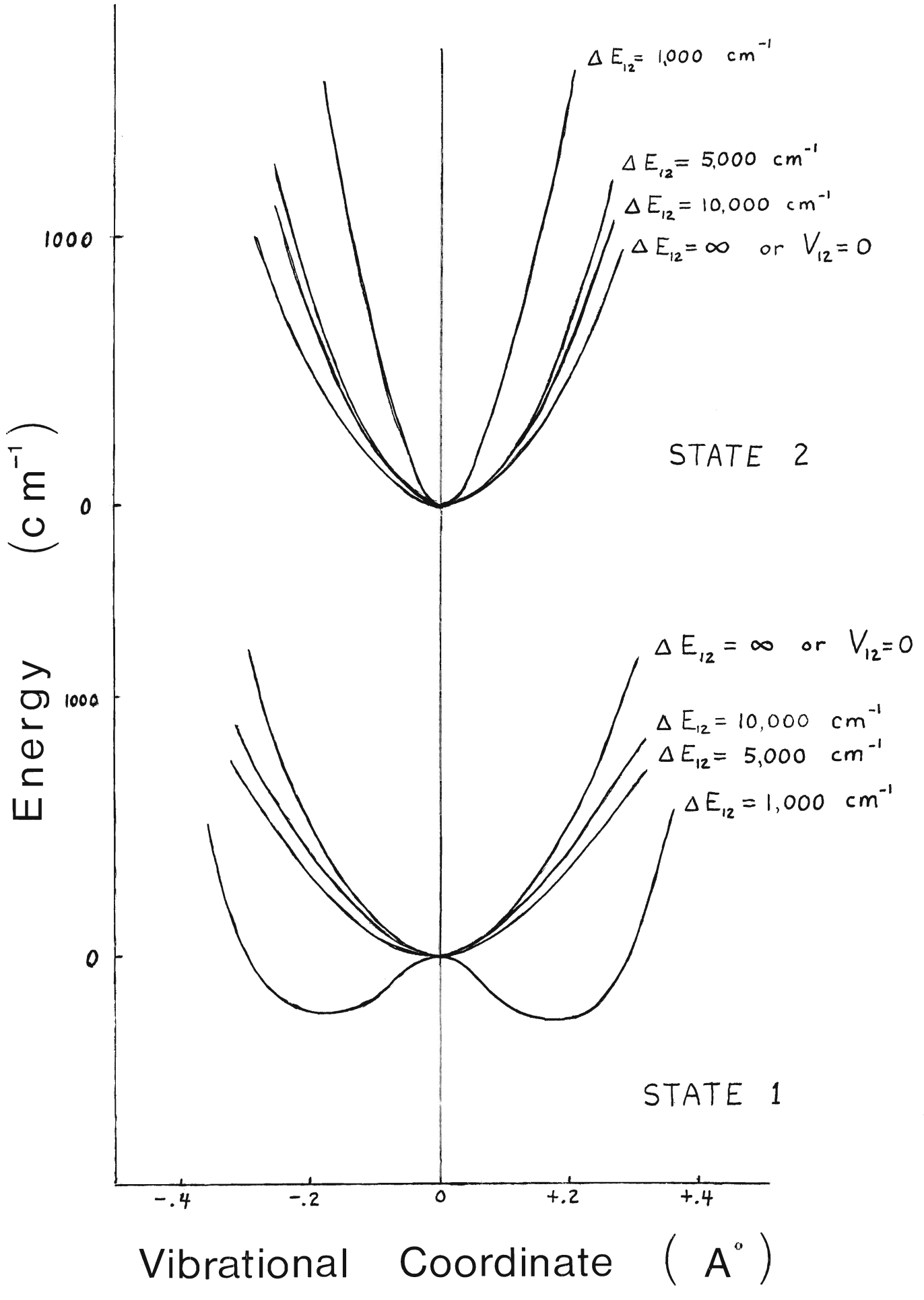
ΔE12 = 1,000 cm-1
ΔE12 = 5,000 cm-1
ΔE12 = 10,000 cm-1
ΔE12 = ∞ or V12 = 0
STATE 2
ΔE12 = ∞ or V12 = 0
ΔE12 = 10,000 cm-1
ΔE12 = 5,000 cm-1
ΔE12 = 1,000 cm-1
STATE 1
1000
0
1000
0
Energy (cm-1)
-.4
-.2
0
+.2
+.4
Vibrational Coordinate (A°)